AD-A141 340 STUDY OF FIELD ALIGNED PLASMA ACCELERATION DURING A 1/1
HANE(HIGH ALTITUDE NU..(U) BERKELEY RESEARCH ASSOCIATES
INC CA S H BRECHT ET AL. 01 MAR 83 PD-BRA-83-288R
UNCLASSIFIED DNA-TR-82-96 DNA001-82-C-0226 F/G 20/9 NL

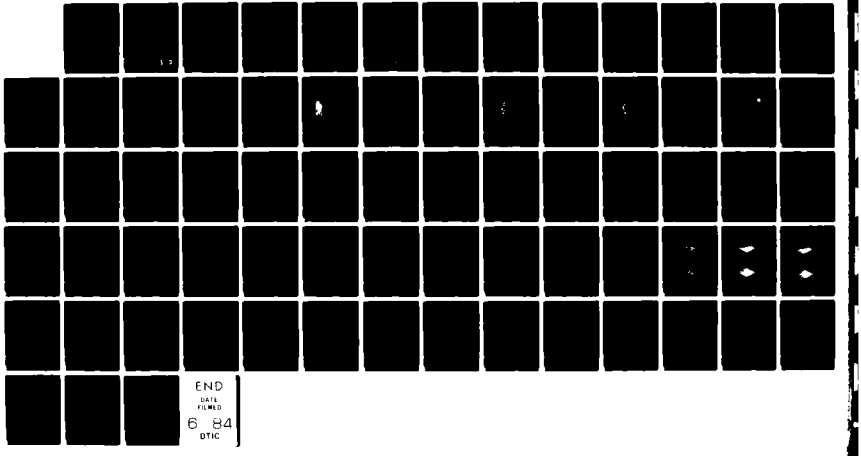

END
DATE FILMED
6 84
DTIC

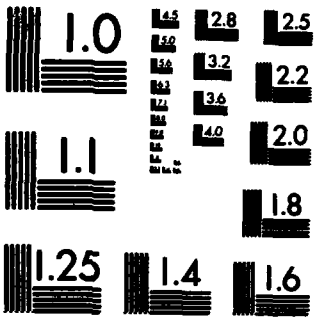

(12)

DNA-TR-82-96

STUDY OF FIELD ALIGNED PLASMA ACCELERATION DURING A H.A.N.E.

Stephen H. Brecht
Joseph H. Orens
Berkeley Research Associates
P.O. Box 983
Berkeley, California 94701

1 March 1983

Technical Report

CONTRACT No. DNA 001-82-C-0226

THIS WORK WAS SPONSORED BY THE DEFENSE NUCLEAR AGENCY
UNDER RDT&E RMSS CODE B322082466 S99QAXHC00064 H2590D.

Prepared for
Director
DEFENSE NUCLEAR AGENCY
Washington, DC 20305

Destroy this report when it is no longer needed. Do not return to sender.

PLEASE NOTIFY THE DEFENSE NUCLEAR AGENCY, ATTN: STTI, WASHINGTON, D.C. 20305, IF YOUR ADDRESS IS INCORRECT, IF YOU WISH TO BE DELETED FROM THE DISTRIBUTION LIST, OR IF THE ADDRESSEE IS NO LONGER EMPLOYED BY YOUR ORGANIZATION.

UNCLASSIFIED

SECURITY CLASSIFICATION OF THIS PAGE (When Data Entered)

REPORT DOCUMENTATION PAGE		READ INSTRUCTIONS BEFORE COMPLETING FORM
1. REPORT NUMBER DNA-TR-82-96	2. GOVT ACCESSION NO. ADA141340	3. RECIPIENT'S CATALOG NUMBER
4. TITLE (and Subtitle) STUDY OF FIELD ALIGNED PLASMA ACCELERATION DURING A H.A.N.E.		5. TYPE OF REPORT & PERIOD COVERED Technical Report
		6. PERFORMING ORG. REPORT NUMBER PD-BRA-83-288R
7. AUTHOR(s) Stephen H. Brecht Joseph H. Orens		8. CONTRACT OR GRANT NUMBER(s) DNA 001-82-C-0226
9. PERFORMING ORGANIZATION NAME AND ADDRESS Berkeley Research Associates P.O. Box 983 Berkeley, California 94701		10. PROGRAM ELEMENT, PROJECT, TASK AREA & WORK UNIT NUMBERS Task S99QAXHC-00064
11. CONTROLLING OFFICE NAME AND ADDRESS Director Defense Nuclear Agency Washington, DC 20305		12. REPORT DATE 1 March 1983
		13. NUMBER OF PAGES 70
14. MONITORING AGENCY NAME & ADDRESS(if different from Controlling Office)		15. SECURITY CLASS (of this report) UNCLASSIFIED
		15a. DECLASSIFICATION/DOWNGRADING SCHEDULE N/A since UNCLASSIFIED

16. DISTRIBUTION STATEMENT (of this Report)

Approved for public release; distribution unlimited.

17. DISTRIBUTION STATEMENT (of the abstract entered in Block 20, if different from Report)

18. SUPPLEMENTARY NOTES

This work was sponsored by the Defense Nuclear Agency under RDT&E RMSS Code B322082466 S99QAXHC00064 H2590D.

19. KEY WORDS (Continue on reverse side if necessary and identify by block number)

Nonlinear Plasma Interactions
H.A.N.E. (High Altitude Nuclear Explosion)
Particle Simulation
Energy Deposition
Field Aligned Acceleration

20. ABSTRACT (Continue on reverse side if necessary and identify by block number)

Research was undertaken to determine if field aligned accleration of plasma will occur following a high altitude nuclear detonation, H.A.N.E. This report represents the preliminary phase of the research. Particle codes were used to study this nonlinear problem in one and two and one-half dimensions using the electrostatic limit. Examination of beam plasma interaction in one dimension showed the expected diffusion of plasma to high energy consistent with previous research. The two and one-half dimension simulations were performed where a loss cone in the velocity distribution was studied. These simulations

DD FORM 1 JAN 73 1473 EDITION OF 1 NOV 65 IS OBSOLETE

UNCLASSIFIED

SECURITY CLASSIFICATION OF THIS PAGE (When Data Entered)

20. ABSTRACT (Continued)

indicated that the loss cone distribution does not appear to be energetic enough to acclerate plasma along magnetic field lines with superthermal velocity.

PREFACE

This is the final technical report on contract DNA001-82-C-0226 covering the reporting period May 1982 through December 1982. The purpose was to examine non-linear plasma interactions to determine the possible mechanisms which might produce field aligned plasma with superthermal energy spectrum.

It is with great pleasure that we acknowledge the assistance of Dr. John Ambrosiano and Mr. John Ferrante. One of us (SHB) would also like to acknowledge the many discussions which have occurred over the years with Drs. R.W. Clark, K. Papadopoulos and P.J. Palmadesso.

TABLE OF CONTENTS

LIST OF ILLUSTRATIONS

LIST OF ILLUSTRATIONS (Concluded)

SECTION I

INTRODUCTION

The shape of the energetic plasma spectrum produced when the expanding debris from a high altitude nuclear detonation interacts with the background plasma has been under study and discussion for years. The component of the energetic particle distribution parallel to the magnetic field is particularly important to questions concerning the location of the ionized deposition region, the level of ionization and the duration of the ionization. The answers to these questions are necessary to do an adequate job of modeling a high altitude nuclear event (H.A.N.E.) and the subsequent systems evaluations performed with these models.

Researchers have addressed the problem of field aligned acceleration of plasma in the past. Clark and Papadopoulos[1] looked into this problem in 1976 and decided that the Post-Rosenbluth[2], loss-cone instability would preferentially scatter particles with perpendicular velocities of about 2.5 times the thermal velocity into the parallel direction. This would create a very energetic spectrum coming down the field lines. They addressed the nonlinear three-wave coupling of waves excited by the Post-Rosenbluth[2] instability and examined the creation of a superthermal tail on the distribution. Then an estimate was made of the amount of energetic plasma scattered from the perpendicular direction into the parallel direction. Most of the nonlinear analysis was performed assuming that the plasma was low beta, i.e., $\beta = 8\pi nkT/B^2 < 1$. A model of this process was created and used in the NRL codes for early time

simulations. It should be noted that in coupling regions of expanding debris, the plasma beta is expected to be greater than one.

It was later estimated by Palmadesso[3] that the simple inverse mirroring effects would also help turn particles from a perpendicular direction to a parallel direction and would preferentially turn particles with velocities above the debris streaming velocity. This work assumed that the magnetic moment of the particle is conserved during the transit down the magnetic field line. This assumption could be severely weakened by the turbulence expected to exist as well as electromagnetic waves that might be anticipated in a high beta system.

Mission Research Corporation has also performed early time H.A.N.E. calculations in the MHD limit.[4,5] The results from their codes predict a much less energetic spectrum coming down the field line. The differences in the NRL and MRC spectrums produce noticeably different results in codes which do chemistry based on the level of ionization produced by plasma streaming down the field lines and depositing in the atmosphere.

There are a host of reasons for the different results and different approaches taken by MRC and NRL. Most of them are based on how the respective groups perceived the evolution of the interaction of the streaming energetic debris with the background ambient plasma. The energy spectrum of plasma coming down the magnetic field is a diagnostic for the larger picture of this interaction.

If one assumes, as MRC does and must because of the MHD approach, that the pickup of plasma and magnetic field is caused by Lamor coupling, then one is constrained to have large scale effects. Any "model" for turning plasma transport and energy into the magnetic field direction which is based on a fluid approach especially a one fluid approach will produce a plasma distribution with a maxwellian shape centered about the local zero parallel velocity. This occurs because of momentum and energy conservation requirements and the limited number of degrees of functions in a one fluid approach.

The opposite view is one where the plasma is not a fluid but exhibits a collisionless behavior. This necessitates a different approach to the dynamics. Here one might expect, wave-particle and wave-wave interactions with large magnetic field compressions occurring in a much smaller interaction length[6,7] than from a fluid approach. The enhanced field compression and small interaction region may allow the magnetic field to play a major role in momentum conservation of the particles being scattered. If the field does take up appreciable momentum in the scattering process that is supposed to send particles down the magnetic field lines, the spectrum of such particles may hold little resemblance to that expected from the usual MHD approach. It is implicitly assumed by NRL in their previous work that this takes place. The upshot of this preferential scattering is an energetic plasma system and the maintenance of the loss cone distribution to do the scattering. The difficulty here is that in order to maintain the loss cone distribution and not end up with a lot of plasma moving in $v_\parallel$ space with the velocity of the magnetic field lines one must have a scattering mechanism that behaves as if the scattering is reasonably

inelastic. This may occur but probably only if the compressed magnetic field region is actively involved in the scattering process such as through electromagnetic waves. There has been some work by Clark et al.[6,7] which indicates magnetic compression of the sort mentioned might exist. However, all of this work has been in one dimension and the 1-D aspect limits the mechanisms for relaxation of the field compression as well as explaining little about the parallel dynamics.

Because of this divergence in views and the importance of the plasma distribution coming down the field line to calculations of ionization, structure, recombination chemistry and emissions such as IR emission, we have undertaken an investigation of whether or not there will be particle acceleration down the field lines.

This report will be limited to research performed on the loss cone type of mechanism. The research is being carried out with one and two dimensional particle codes. The results to be discussed in this report are from the electrostatic versions of these codes. We will discuss not only the results of the simulation work but the validity of the model. In addition we will comment on the role of the loss cone mode in the H.A.N.E. environment as well as where it is likely to be found.

The report is organized into five sections. Section II will present our numerical methods and the parameters used in simulations. In Section III a synopsis of the relevant theory dealing with the loss cone mode is presented. The fourth section is devoted to the results of the simulations themselves. In the

last section we will summarize and discuss our conclusions from this research and provide some guidelines to where it should proceed from this point.

SECTION II

NUMERICAL METHODS

The basic tool used in this research is the particle code in one and two dimensions. It differs from, for instance, an MHD code in that only the Lorentz force is applied to the individual particles which populate the grid. The particle response is collisionless in the classical sense. More importantly, the particle simulation allows kinetic phenomenon such as wave-particle and wave-wave interactions to occur. This permits simulation of small scale (less than a gyroradius) collisionless interaction, something that by the very assumptions used to obtain the MHD equations is proscribed in an MHD code.

The H.A.N.E. problem is obviously three dimensional but because of the usual computer limitations (size and speed) the best we can hope to achieve is a 2 1/2 dimensional simulation (three velocities and two spatial dimensions). We are interested in the field aligned acceleration aspect of the total problem, therefore we have selected the $\bar{x}$ direction to be the expansion direction across the magnetic field while the $\bar{z}$ direction is taken to be along the magnetic field.

The usual loss cone analysis assumes $k_{||} << k_{\perp}$ and only addresses the quasilinear effects of the perpendicular electric field. We are looking for acceleration down the field line and must consider the possibility that the modes of interest may have a significant parallel electric field. For such fields

to occur the parallel wavelength shall be sufficiently long so that electron Landau damping is negligible ($\omega >> k_{||} v_{||}$).

The requirement that $\lambda_{\perp} << \lambda_{||}$ produces a considerable hardship for a particle simulation because in the simplest of particle codes one cannot have cell sizes much larger than the electron debye length (λ_{De}). But to avoid the electron Landau damping one needs waves in the system from (10 to 200) λ_{De} in the parallel direction. This is impossible if one is to resolve the perpendicular direction adequately enough to see the predicted nonlinear behavior.

We have greatly expanded the limit on the grid size by going to a more complex interpolation scheme in the code, doing filtering of the k-space electric fields and using particles of macroscopic size (larger than a perpendicular cell size). The interpolation scheme selected and the particle shape used is that of a cubic spline. The actual shape function has the following form:

$$S_3(x) = \begin{cases} 2/3 - x^2(2 - |x|)/2 & |x| \leq 1 \\ (2 - |x|)^3/6 & 1 \leq |x| \leq 2 \\ 0 & |x| \geq 2 \end{cases} \qquad (1)$$

where x denotes the displacement of the individual particles from the surrounding grid points. Basically the cubic spline interpolation is used to distribute the particle charge over the grid and to apportion the resultant electric fields to the particle positions. A cubic spline Fourier-space particle shape factor is

applied to smoothly cut off the k-spectrum and preserve integrity in real space. A smooth cut-off of the spectrum is important since much of the numerical grid noise is carried by wavelengths on the order of the grid spacing (largest k-modes). An abrupt cut-off with

$$S(u) = \begin{cases} 1 & |u| \leq 2 \\ 0 & |u| > 2 \end{cases} \qquad (2)$$

where $u = k/(1/2\ k_{max})$, would yield a real-space particle shape in the form of a sinc function $\left[\sin(1/2\ rk_{max})/(1/2\ rk_{max})\right]$ which has the undesirable property of negative "ringing" attenuated only as $1/r$. Cubic splines go as $sinc^4$ and produce a $1/r^4$ attenuation. The result of the cubic spline approach which is costly on a per particle basis is that we can use grid cells of 10 to 40 λ_{De} in the parallel direction. We have in fact done simulation tests to make sure that the grid effect problem has been reduced to a negligible level, and have found this to be the case.

The one and two and a half dimension simulations reported here are electrostatic in nature. In the 1-D code we used a 256 cell mesh where each cell was 2 λ_{De}. A series of tests were run looking at the behavior of a counter streaming ion beams using 1, 4, 8, 16 particles per cell. The purpose was to determine how many particles/ cell were necessary for an adequate simulation. The effect of too few particles can be seen in Figures (1-2) where in addition to the relaxation of the distribution to a more maxwellian shape particle acceleration was also

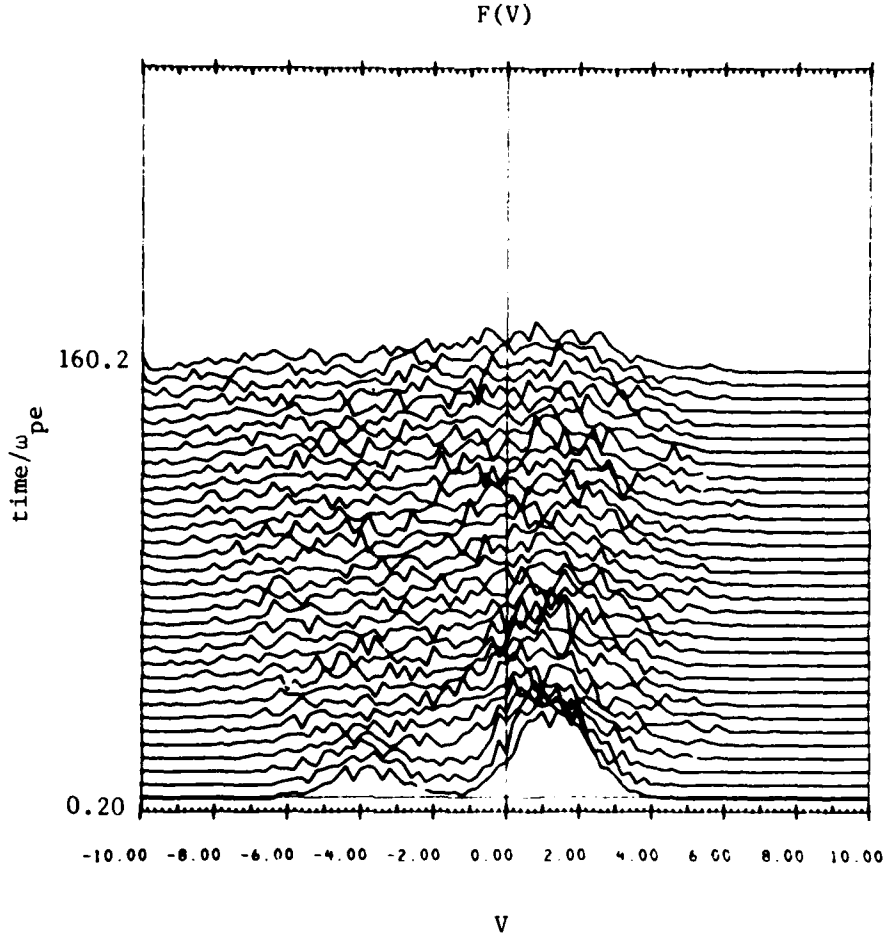

Figure 1. A histogram of the ion distribution function for a run of 4 particles/cell. Note scattering to high positive and negative velocities, this occurs because of numerical noise in the system.

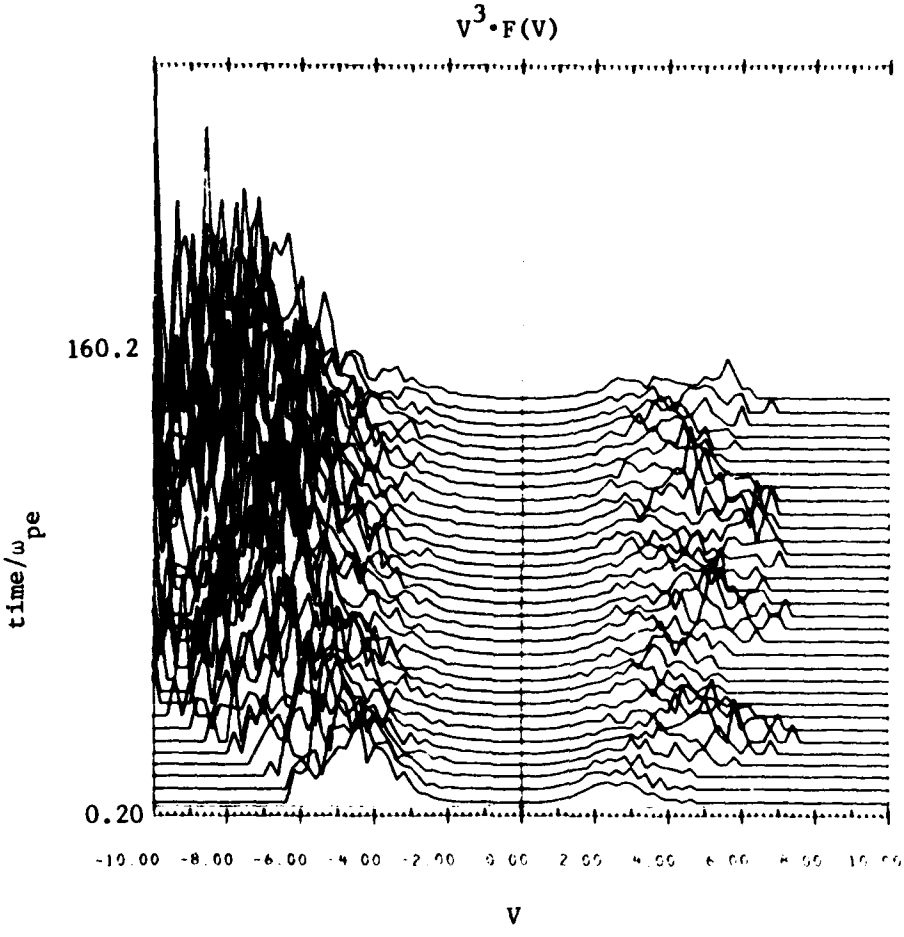

Figure 2. A histogram of the ion energy flux for a run of 4 particles/cell. This shows the large change in energy flux caused by the numerically generated diffusion in the simulation.

seen in the high energy tail of the distribution due to spurious electric fields. At 8 particles/cell the numerical effects are greatly reduced (Figures 3-4) and at 16 particles/cell (Figures 5-6), the whole simulation was extremely quiet. For the work to be discussed in this report 8 particles/cell were selected.

The 2 1/2-D code used an x, z grid of 128 by 32 cells where in the $\hat{x}$ direction the cell size is 2 λ_{De} and in the parallel direction the cell size is 40 λ_{De}. In both codes the nominal mass ratio m_i/m_e is 64/1. For the actual H.A.N.E. simulation it was assumed that the loss cone distribution would be maintained as discussed in Clark and Papadopoulos.[1] Therefore an algorithm was placed in the code which tends to maintain the loss cone. The importance of maintaining this form will be discussed in the next section. Also a review of theory will be presented in that section.

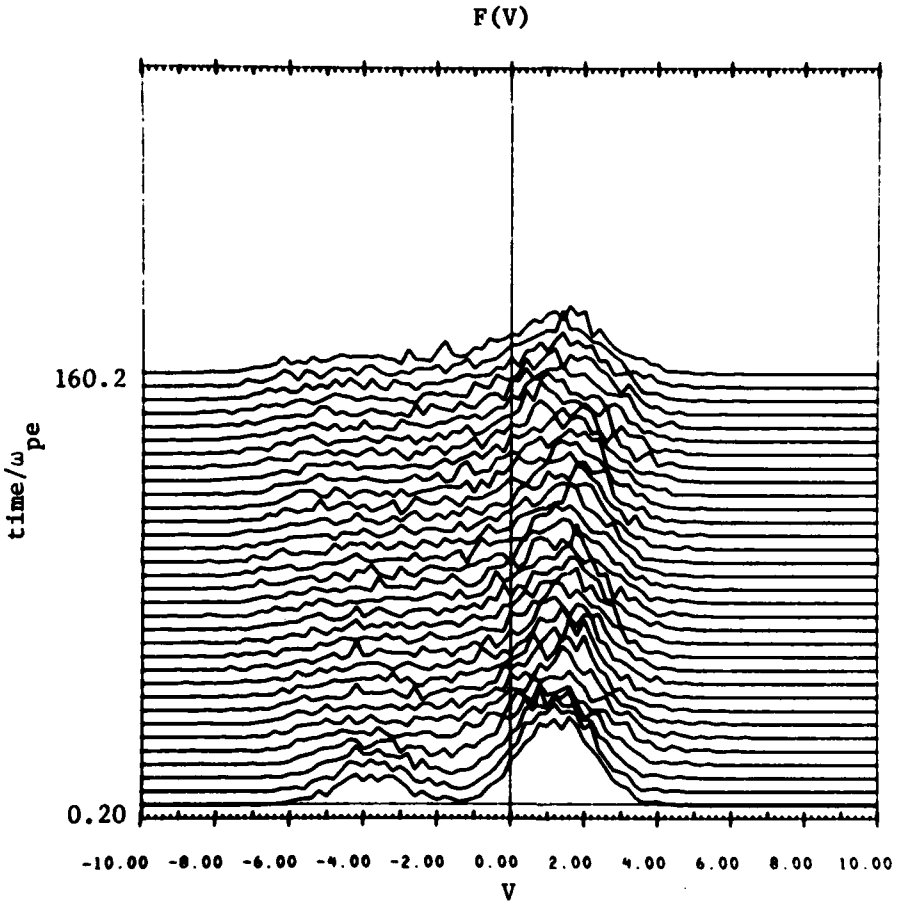

Figure 3. A histogram of the ion distribution function for a simulation with 8 particles/cell. The noise has been substantially reduced and much less scattering occurs particularly in the larger maxwellian distribution.

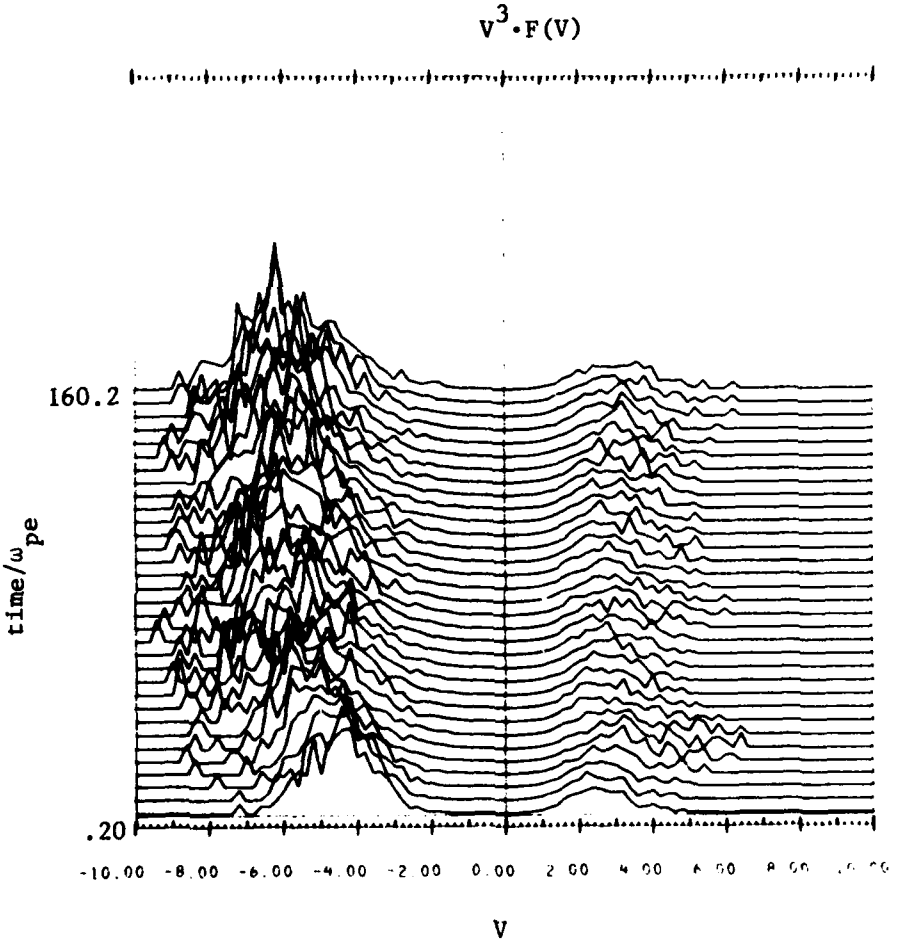

Figure 4. A histogram of the ion energy flux for 8 particles/cell. The amount of diffusion to high energies has been significantly reduced but is still in evidence.

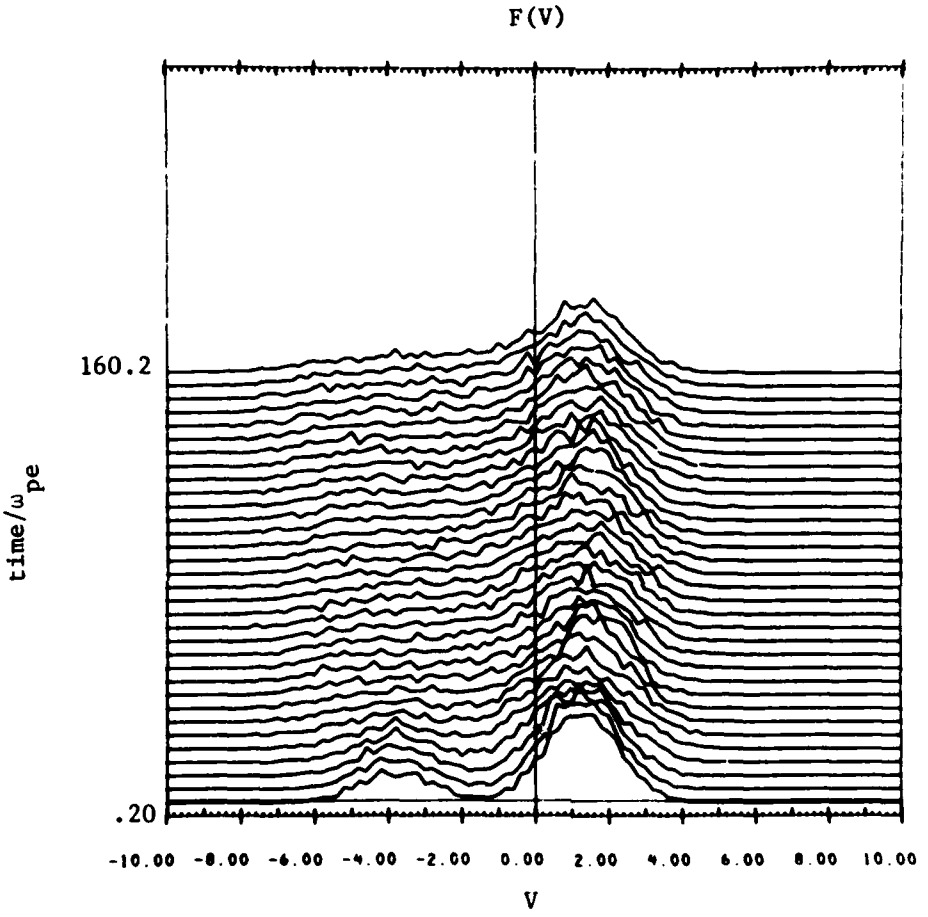

Figure 5. A histogram of the ion distribution function for a simulation with 16 particles/cell. It is quieter than is seen in Figure 4 but only marginally.

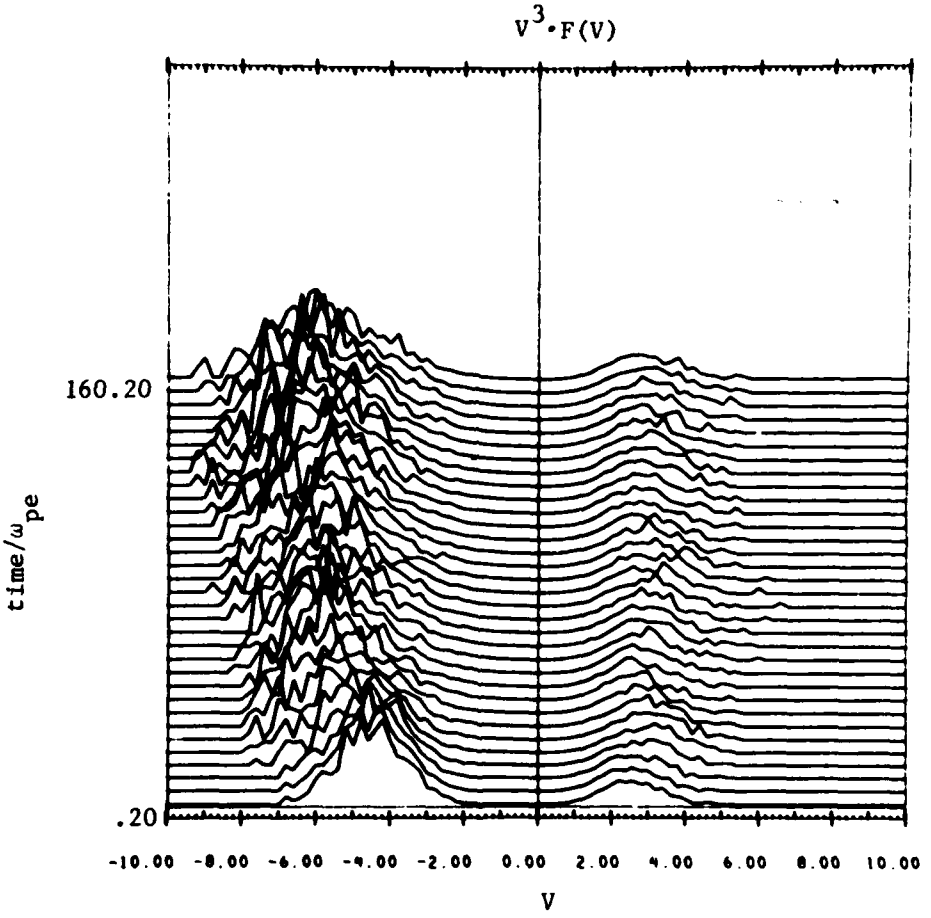

Figure 6. The histogram of the ion energy flux for 16 particles/cell. The amount of diffusion seen here is essentially the same as Figure 4.

SECTION III

THEORY

The term loss cone instability is actually applied to a larger class of instability than is found in a magnetic mirror machine. In the DNA community the term loss cone also refers to a physical region in the perturbed magnetic field where plasma simply streams down the magnetic field lines. The loss cone instability is often applied to situations where there is a deficiency in the parallel part of the distribution through loss or enhancement of a portion of the perpendicular velocity space such that a gradient in the distribution $f(v_\perp, v_{||})$ is produced (Figure 7). Unstable loss cone distributions $\frac{\partial f^{ion}}{\partial v_\perp}(v_\perp, v_{||}) > 0$, are found in the fusion devices such as magnetic mirror machines (Gerver[8] and Cohen[9]) and tokomaks where neutral beam injection is taking place, Hitchcock et al.[10] They exist in the ionosphere particularly in the polar region and in the magnetosphere. This instability is predicted to play a critical role in the Southern Conjugate rebrightening seen in Starfish, Brecht et al.[11,12]. Of most importance to this work, the loss cone instability was predicted by Clark and Papadopoulos[1] to produce in its nonlinear evolution an acceleration, or perhaps scattering is a better word, of high energy plasma down the magnetic field line during a H.A.N.E.

The linear analysis that is traditionally performed assumes that L, the macroscopic scale length, i.e., the length of the field line, is large compared to

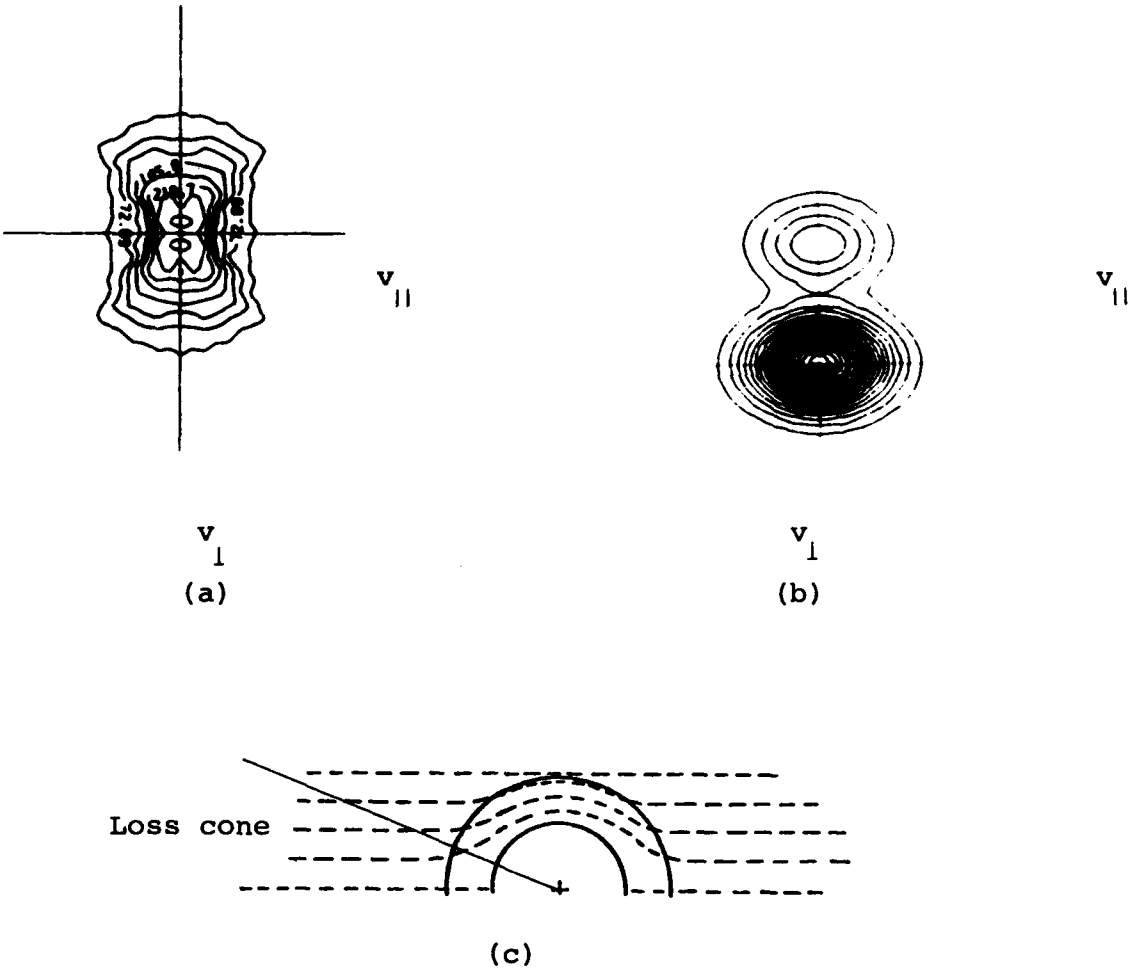

Figure 7. a) This is the typical distribution found in mirror geometries. This distribution occurs in mirror machines and at the ends of geomagnetic field lines.

b) This is a distribution often termed loss cone produced by an unmagnetized plasma beam interacting with a maxwellian background.

c) This is the loss cone region often referred to in H.A.N.E. work. This geometry is the same as the mirror machines.

the wavelength, $\lambda_{||}$, of the loss cone. This assuption, $L > \lambda_{||}$, is made so that the mode has sufficient room to grow as it propagates down the magnetic field line. A second assumption is that $k_{\perp} >> k_{||}$ where $k \equiv 2\pi/\lambda$. Also it is generally assumed that the frequency of the wave, ω_k, is much greater than the ion cyclotron frequency, $\omega_{ci} \equiv \frac{eB}{mc}$ and that $k_{\perp}^2 \rho_i^2 >> 1$ where ρ_i is the ion gyroradius. This assumption means that to first order at least the ions are unmagnetized; a good assumption in the early time H.A.N.E.

A further assumption about the electrons is usually made and that is $|\omega_k| << |\omega_{ce}|$ and $k_{\perp}^2 \rho_e^2 << 1$ (the electrons are magnetized). This assumption can be relaxed and will need to be in the H.A.N.E. case. The relaxation of this assumption only reduces the growth rate by $1/(1 + \omega_{pe}^2/\omega_{ce}^2)^{1/2}$ where ω_{pe} is the plasma frequency, $\equiv \left(\frac{4\pi ne^2}{m_e}\right)^{1/2}$. In its simplest form the real frequency of the loss cone instability for high velocities is found to be

$$\omega_k \sim \frac{k_{||}}{k} \omega_{pe} \tag{3}$$

with a growth rate that is approximately

$$\gamma \sim \frac{\omega_{pe}}{2} \left(\frac{\omega_k}{k\bar{v}}\right) \delta\left(\frac{\omega}{k\bar{v}}\right) \tag{4}$$

where $\delta(\omega/k\bar{v})$ is a sinusoidal function with argument $(\omega/k\bar{v} - \pi)$ and $\bar{v}$ is the mean thermal speed.

As shown by Davidson[13] and Galeev[14], the nonlinear evolution of the loss cone instability diffuses particles

into the loss cone region and thus stabilizes the wave by reducing $\frac{\partial F}{\partial v_\perp} \rightarrow 0$. However, if the loss time, t_ℓ, out of the system, i.e., down the field line, or plasma replenishment time, t_r, is such that cold plasma in the moving magnetic field frame of reference in the H.A.N.E. case is interacting with the system faster than the non-linear diffusion time, t_D, the loss cone instability will persist; t_r or $t_\ell < t_D$. If such a situation exists then, as pointed out by Galeev[15], the only way for the unstable modes to limit themselves is through mode coupling to a mode that has a plasma velocity, ω/k, that matches a portion of the distribution $\frac{\partial F}{\partial v_\perp} < 0$ where it will damp and place the energy back into the distribution. This produces a diffusion of the negative slope of the ion distributions to high energy. Clark and Papadoupoulos[1] pointed out that such a case could exist for a H.A.N.E. They theorized that if this nonlinear state were reached then particles with high velocity would be scattered off of the high phase velocity waves down the magnetic field line. They arrived at an estimate of 2.5 v_{thi} as the average scattering velocity, where v_{thi} is the ion thermal velocity.

However, if one considers the type of plasma parameters predicted by the multifluid code, KLYSMA[6], in the interaction region, one finds that for oxygen or aluminum that v_{thi} at 15 keV is approximately 2.5-5 times less than the expected 2×10^8 streaming velocities and therefore the modes driven unstable by the loss cone could provide the scattering parallel to the magnetic field line but would not provide particles moving faster than the original expansion velocity. However, the estimated phase velocity of these waves

parallel to the field line does approach the electron thermal velocity. Therefore, scattering by such waves may produce velocities approaching the parallel phase velocity and be even more energetic than predicted by Clark and Papadopoulos.[1]

One of the interesting aspects of the current loss cone mode analysis is that most of the nonlinear treatments only consider the perpendicular diffusion coefficient. However, the existence of a finite $k_{||}$ is in fact postulated and used to estimate growth along the magnetic field line. Therefore one in fact has an $E_{||}$ associated with the mode. This $E_{||}$ driven to sufficiently high levels by nonlinear waves could provide the predicted scattering.

All of this discussion leads to the basic reason we are performing this research. There appears to be several possible mechanisms by which the loss cone instability might provide an energetic field aligned spectrum. The pure scattering mentioned by Clark and Papadopoulos, nonlinear energy diffusion in the mode spectrum allowing parallel propagation waves to scatter particles, or electromagnetic responses due to inhomogeneous magnetic fields are all candidates. If any of these mechanisms work, it is through a very nonlinear interaction between various waves and the distribution function. The analysis drawn from data is only an approximation, therefore in order to determine what actually does occur when a loss cone distribution is driven to a nonlinear state we have chosen to simulate it with a particle code.

In the next section we will discuss these simulations performed to date and their results.

SECTION IV

SIMULATION

During the course of the contract two sets of simulation codes were utilized; a 1-D cubic spline code and a 2 1/2-D cubic spline code. The 1-D code was built and used as a test bed to develop numerical algorithms and to determine appropriate physical parameters. Once the appropriate determinations were made for numerical and physical parameters the 2 1/2-D code was used to study the loss cone problem.

The 1-D code was run with 256 cells and 8 particles/cell. The cell size decided upon was $\Delta x = 2\ \lambda_{De}$. All of the tests were run with the one dimension perpendicular to the magnetic field. The initial distributions for these runs were maxwellian electrons and ion distributions of the form shown in Figures 1, 3 or 5. Initially fusion type parameters were run with both ions and electrons magnetized. Later only the electrons were magnetized, $\omega_{ce}/\omega_{pe} \sim 2$, and the ions free streamed consistent with the H.A.N.E. situation. The ions were loaded onto the simulation grid as two maxwellians of 10 keV temperature. One quarter were loaded into one distribution and three quarters into the other. A relative drift of five times the ion thermal velocity was imparted to the test distribution similar to possible H.A.N.E. situations. This gave a center of mass velocity of 3.75 times the thermal velocity. As can be seen in Figure 3 the initial distribution was not that of a classic loss cone in $v_\perp$ space, but was more the beam plasma type of distribution. After $t \sim 10/\omega_{pe}$ the diffusion caused by the instabilities in the plasma have

created a loss cone like distribution as seen from the response of non-drifting distribution. From here on the evolution should follow that of a loss cone distribution. One important point to be made here with regard to all these distributions is that the classic loss cone analysis assumes a distribution function which is symmetric about the magnetic field. Until one reaches times of ~ 0.01 second or longer after the debris and air interaction begins such assumptions for the H.A.N.E. case (Starfish) are not appropriate. More discussion on this topic is forthcoming in the conclusion section of this report.

A variety of mundane but important parameters were tested with the 1-D code. The effect of the ion/electron mass ratio was tested by varying the ratio from 16/1 to 128/1 in powers of two. This showed, as expected from theory, that the effects seen in the simulation were caused by the ions primarily although the electrons do play a role in the dynamics. The mass ratio decided upon for the major simulation was, 64/1, ion to electron ratio. The effect of grid size was also checked to determine if the size, Δx, of the grid provided both sufficient spectral density and range of k spectrum to allow the expected dynamics such as resonant interaction with the slope of the distribution and three wave mode coupling. The grid of $\Delta x \sim 2\ \lambda_{De}$ was found to be sufficient to represent the appropriate resonance regions as well as allow the nonlinear mode coupling expected; λ_{De} is the electron debye length $\lambda_{De} \equiv v_{the}/\omega_{pe}$. An important result was that one could use a system of 128 cells in the perpendicular direction

and perhaps 64 if necessary and get adequate resolution with a periodic system. This information was particularly important when the 2 1/2-D code was to be used because we then knew that 128 cells in a doubly periodic system would be sufficient leaving some memory and money to include the second dimension and required number of particles.

Figure 3 demonstrates the dynamic effect the plasma instabilities have on the distribution function. The total time covered in Figure 3 is $160/\omega_{pe}$ where each line drawn represents $\Delta t \simeq 5/\omega_{pe}$. As can be seen from Figure 3 diffusion to high velocities occurred for both distributions, however, the lower density distribution is seen to be completely smoothed out by the end of the run and bears no resemblance to a maxwellian. This occurs because of the center of mass effect. This plot is shown in the systems center of mass which explains why the larger density distribution function is slightly diffused. Note that by $t \sim 20/\omega_{pe}$ strong velocity diffusion has almost filled in the hole between the two distributions. Figure 4 shows the effect of this diffusion on the energy flux of the system. Here one sees a rather substantial shift upward in the energy flux. It should again be emphasized that this was a very energetic beam distribution with two distinct ion species not a thermalized loss-cone distribution with one ion species.

The electric field spectrum behaved as expected. The total electric field energy was approximately ten percent of the thermal energy in the system. The mode, $k = 25$, that resonated with the positive slope of the small beam was excited to high levels as compared to

all other modes. This can be seen in Figure 8 which shows all the modes in the system including the conjugate ones. Because of the periodic boundary conditions the positive and negative modes are identical. In this section the dimensional mode, K_i, is defined as $K_i \equiv \frac{2\pi i}{\Delta x N} = \frac{1}{\Delta x} k$, where N is the number of cells in a specific direction and k is the dimensionless mode number referred to in this section which corresponds to the index, i, i.e., $k = 25$. Also seen in Figure 8 is that $k = 2$, a long wavelength mode with a phase velocity that matches particle velocities far out in the distribution, is the only other dominant mode. These two modes vary dramatically during the simulation as can be seen in Figures 9 and 10. However, only the $k = 25$ mode is obtaining its energy directly from the beam. The long wavelength mode is apparently deriving its energy from nonlinear three wave coupling.

Looking at Figure 10, one can estimate the linear growth rate of mode 25 assuming an exponential growth. Making this assumption a growth rate of $\gamma \sim .12\ \omega_{pe}$ is obtained. Using a maximum entropy technique[16] the fundamental frequency of this mode was determined to be $\omega \sim .08\ \omega_{pe}$. The rate of diffusion and growth for the modes can be checked with theory to determine if the simulation is behaving as quasilinear theory might suggest. Although most of the theory is for a two dimensional system the quasilinear diffusion is generally a one dimensional calculation. Using the work of Sagdeev and Galeev[17] we employ their equation for quasilinear diffusion (II-59)

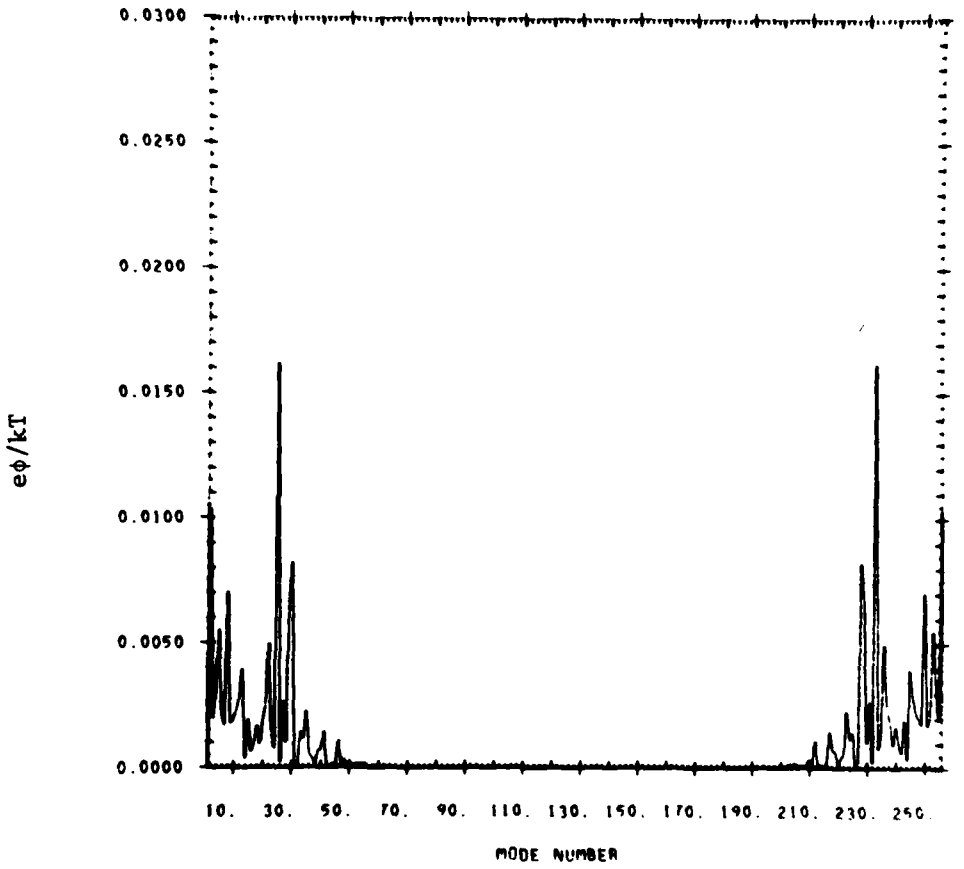

Figure 8. A typical mode spectrum for the one dimensional simulations. Note that most of the energy resides in modes 25 and 2.

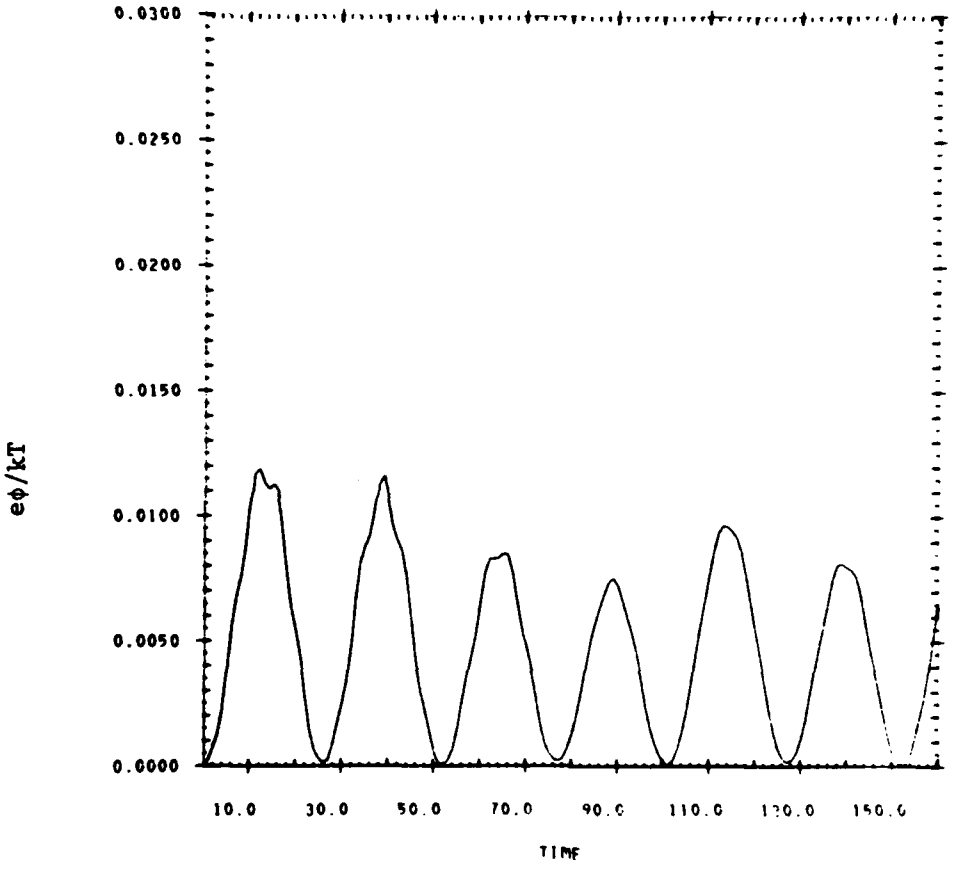

Figure 9. Time evolution of mode two, k = 2.

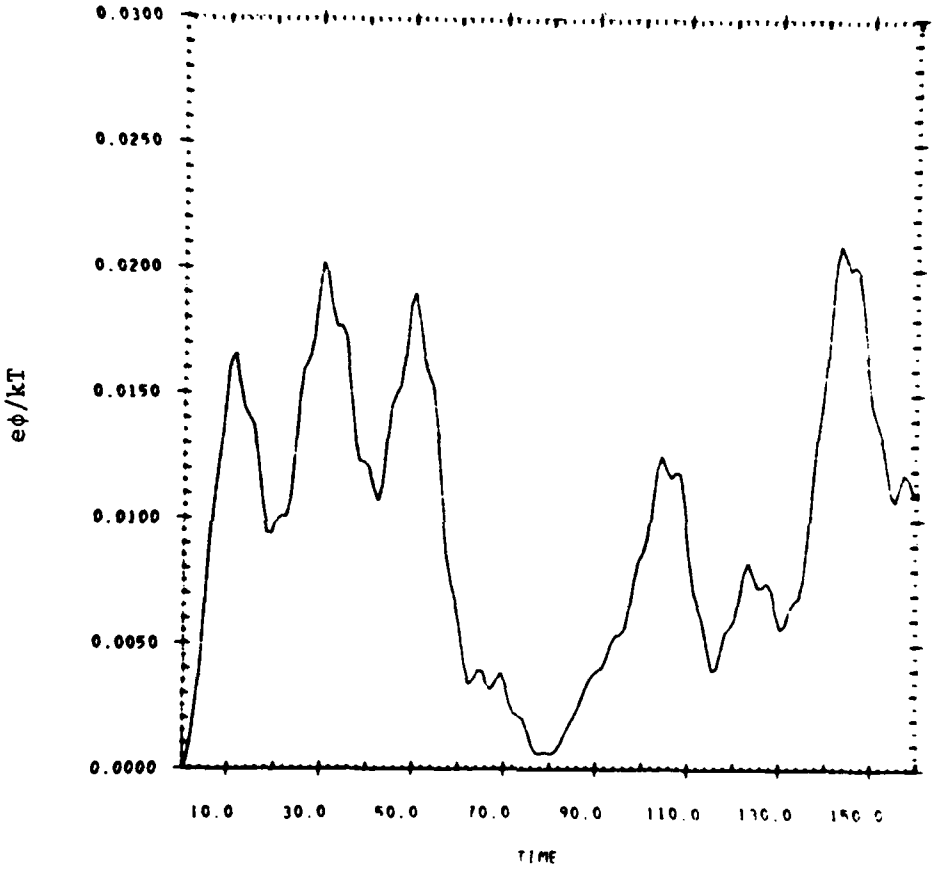

Figure 10. Time evolution of mode twenty five, k = 25.

$$\frac{\partial \psi}{\partial t} = \frac{\partial}{\partial w} \sum_k \frac{|\omega_k| e^2 |\phi_k|^2}{m_i^2 v_{thi}^4 (w/y-1)^{1/2}} \frac{\partial \psi}{\partial w} \qquad (5)$$

where $w = v_\perp^2 / v_{thi}^2$, $y = (\omega_k / k_\perp v_{thi})^2$ and ψ is the distribution function. One can estimate the time necessary for quasilinear diffusion, τ_q, from Eq. (5) by making the following assumptions:

$$\frac{\partial \psi}{\partial t} \sim \frac{\psi}{\tau_q}, \quad \frac{\partial}{\partial w} \sim \frac{1}{\Delta w} \quad \text{and} \quad v_\perp \sim \omega_k / k_\perp .$$

using these assumptions the following relation is obtained:

$$\frac{1}{\tau_q} \sim \frac{|\omega_k| e^2 |\phi_k|^2}{m_i^2 v_{thi}^4 (w/y-1)^{1/2} (\Delta w)^2} \simeq \frac{|\omega_k|^2 v_{thi}^4}{v_\perp k_\perp (\Delta v_\perp^2)^2} \left(\frac{e|\phi_k|}{kT} \right)^2 \qquad (6)$$

A reasonable assumption for $\Delta v_\perp^2$ is that $\Delta v_\perp^2 \sim \frac{v_{thi}^2}{2}$. With this assumption, the information from Figure 10 and the real frequency, τ_q can be evaluated, where we have correctly assumed that $k = 25$ produces most of the diffusion effects. Using this information one obtains the result that

$$\tau_q \sim (.36\ \omega_{pi})^{-1} \qquad (7)$$

This implies that the quasilinear diffusion time varies as $m_i^{1/2}$. This was checked against the runs made with varying mass ratio and found to agree quite well. In terms of the mode data from the 8 particles/cell simulation, $\tau_q \sim 20/\omega_{pe}$ using the 64/1 mass ratio. This is in very good agreement with the data, Figure 3.

In order to determine if nonlinear three wave interaction took place further work with the electric

fields was necessary. Figures 9-11 show the time history of the most important modes. Figure 9 shows the time history of mode two. Note the rapid growth in the energy of the mode. Figure 10 displays the main resonant mode, k = 25. As inferred from Figure 8, this mode has most of the electric field energy. Figure 11 shows mode 27. The data shown on these plots, as well as the other modes, were analyzed to determine their frequencies. A standard FFT was found to be inadequate for this task because of the sparsity of temporal data. Instead we employed a maximum entropy technique[16] which is considerably more sensitive to sinusodial variation in a sequence of data. It was presumed in this analysis that a sinusoidal dependence existed and certainly Figures 9-11 demonstrated that it does for the most part. Because of this assumption and the fact that one uses coefficients to determine the frequency curve, spurious signals can be generated. We used both a 5 and a 25 coefficient curve to check our results. There were differences in the results. Only the frequency with the largest PSD for each mode was considered. One could reasonably expect to see several other modes besides the driven ones in the PSD's and they do appear. The electron plasma oscillation should be present, as well as, the ion plasma frequency, $.25\ \omega_{pe}$, and the electron sound wave with $\omega^2 \lesssim \omega_{pe}^2 + \omega_{ce}^2$. Evidence for all these modes was found.

Using the maximum entropy technique we obtained the required data to check and see if nonlinear wave interactions were occurring. Specifically we looked for waves that met the following criterion for wave-wave interaction:

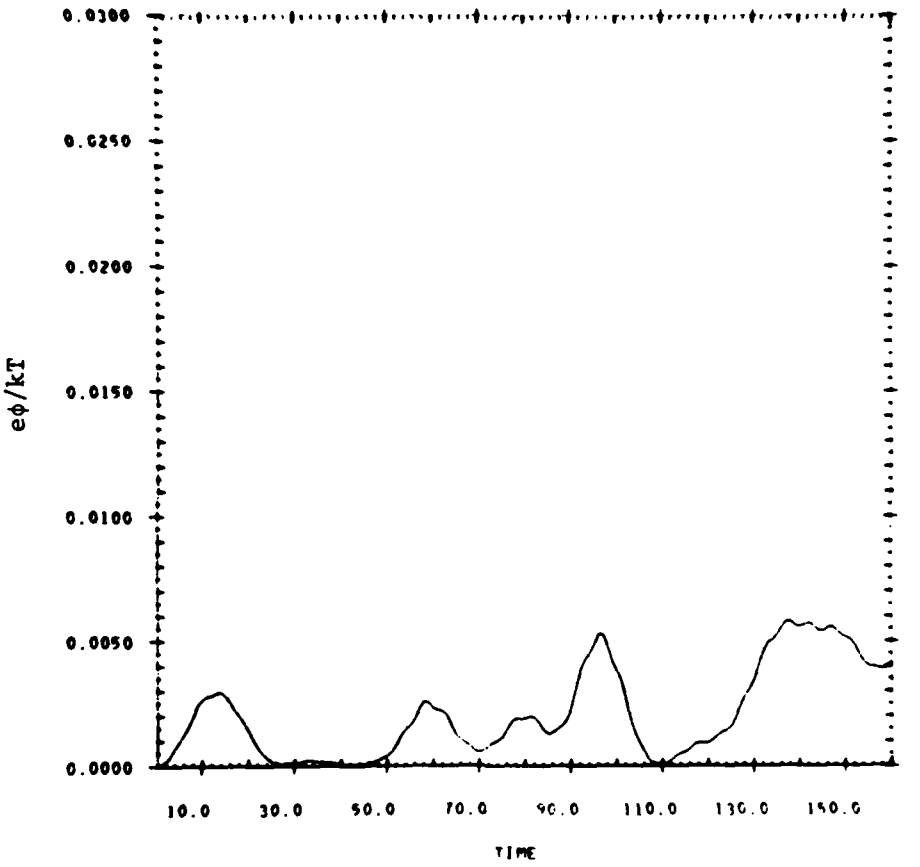

Figure 11. Time evolution of mode twenty seven, k = 27.

$$k_1 + k_2 + k_3 = 0 \tag{8}$$

$$\omega_1 + \omega_2 + \omega_3 = 0 \tag{9}$$

where k and ω may be either positive or negative. Looking at a series of plots like those in Figure 8 gave evidence that mode 2 and 25 might be coupled energetically. In Figures 12, 13 and 14 the frequency dependence of modes 2, 25 and 27 are displayed. It was determined that these modes, 2, 25, and 27, met the appropriate conditions for a three wave interaction, $k_{27} + k_{-25} = k_2$ and $\omega_{27} + \omega_{25} = \omega_2$. More important 27 and 25 grew fast enough to account for the rapid onset of mode 2 as seen in Figure 9. Mode 27 was also found to be driven by the beam distribution but transferred its energy into mode 2. Other three and four wave interactions probably occur in this simulation but because of the rather monochromatic behavior of modes 2 and 25 other relations were not considered here. The main purpose was after all to determine if resonant and nonlinear behavior could occur in the spectral spacing (Δx) and spread ($N\Delta x$) given. Looking at Figure 8 one also notes that most of the dynamics in the electric field occurred in modes 2-35 implying that a 256 cell system with 128 modes and their complex conjugates could be easily handled with a 128 system and 64 unique modes.

An additional set of runs were made where all conditions discussed above were repeated except, that instead of letting the distribution relax normally, a source of plasma was placed into the simulation to represent the effect of cold plasma being constantly

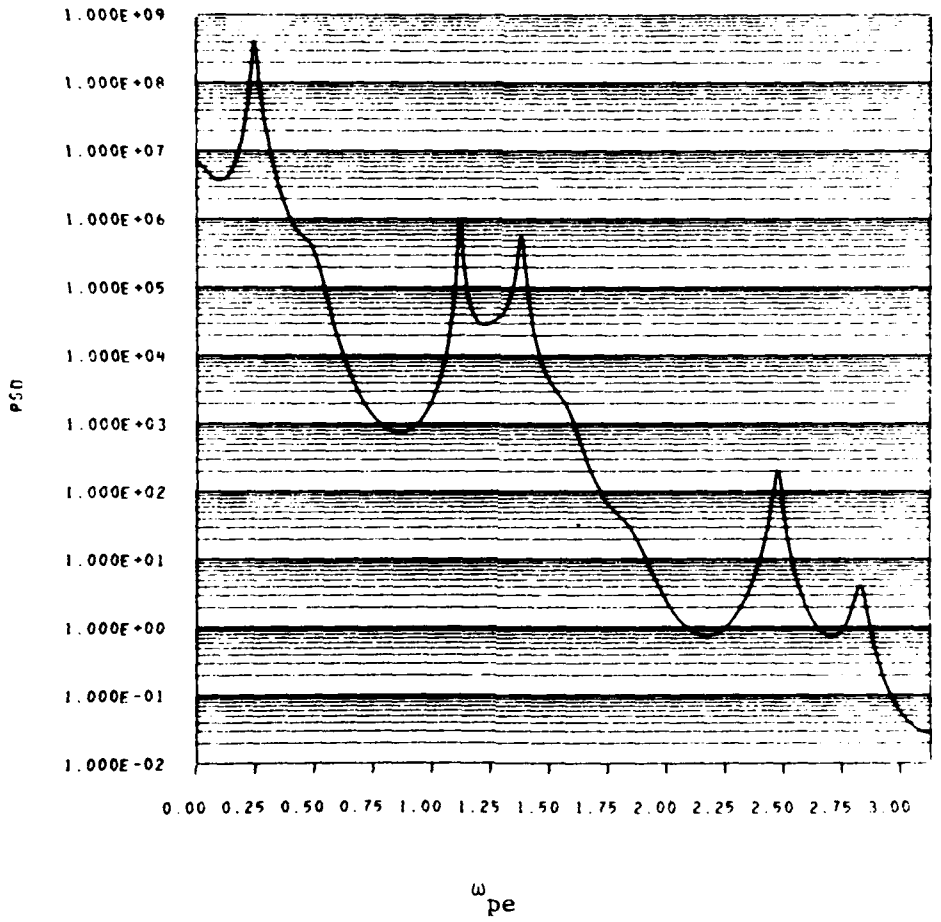

Figure 12. Power spectral density of mode, k = 2.

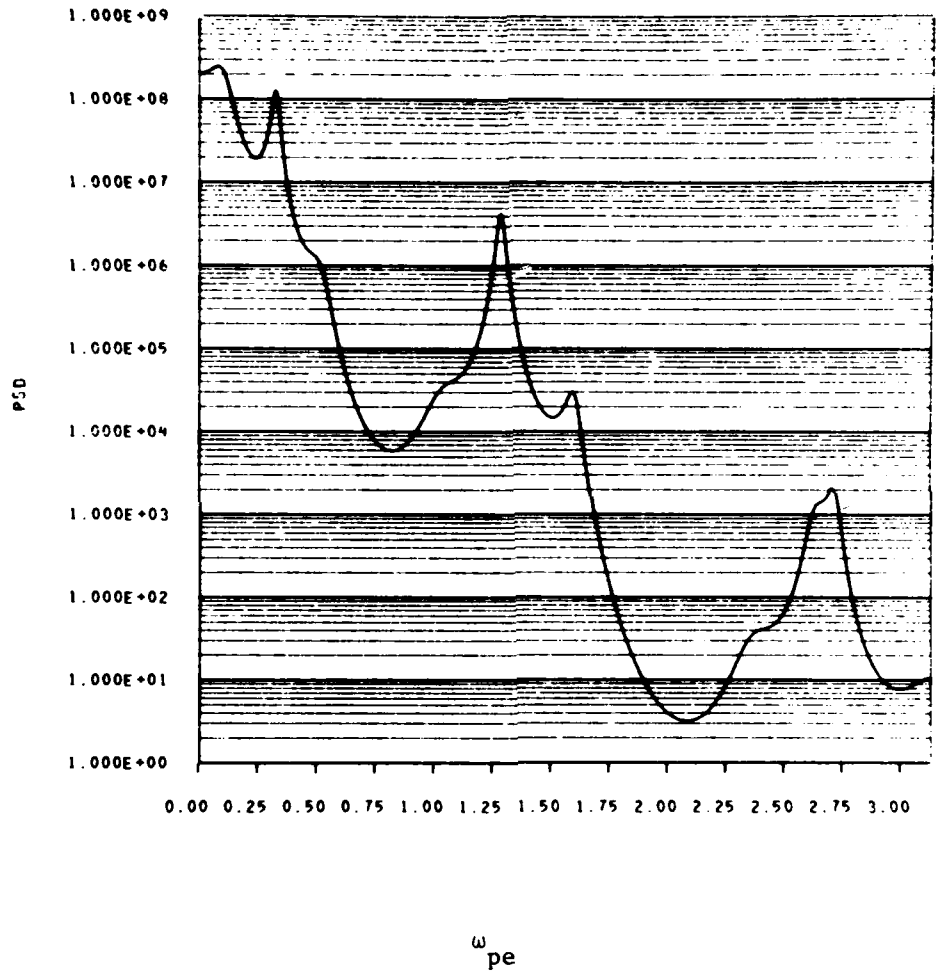

Figure 13. Power spectral density of mode, k = 25.

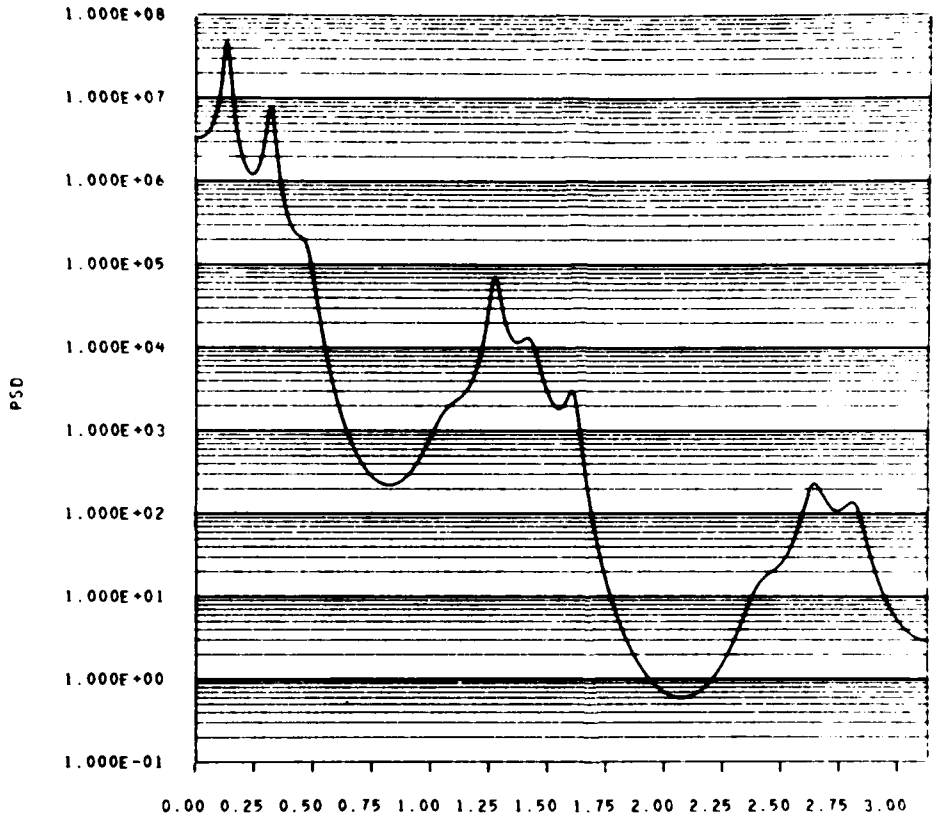

Figure 14. Power spectral density of mode, k = 27.

swept up. To do this an algorithm was developed that attempted to hold the initial distribution fixed. Simply putting particles at a specific velocity will lead to a numerical beaming instability. Instead a random number generator was used to select a given number of particles from the total velocity distribution and randomly redistribute them in velocity space so as to match the original distribution. For the additional simulations approximately 2 particles/step were replaced. This represents a rather high energy replacement compared to the real situation. The results were found to be quite similar particularly in the electric fields. As can be seen by comparing Figure 3 with Figure 15 there is a slight change in the late times with the replenished system maintaining a sharper peak in the beam and producing a sharper PSD.

The 2 1/2-D simulation was carried out on a standard loss cone distribution. This distribution differs from the one dimensional simulation as can be seen in Figure 16. We studied the standard loss cone because it was specifically discussed in the literature as a possible scattering mechanism. The results of the 1-D runs would imply a beam plasma interaction as a likely condidate. However, for thoroughness and completeness we persisted with a thermalized loss cone distribution. In this case there really is only one ion distribution function. The simulation was prepared by loading ions and electrons to represent a 5 keV temperature and an effective mirror ratio of two. This was accomplished with a random number generator as were the 1-D simulations. The equation used for loading was:

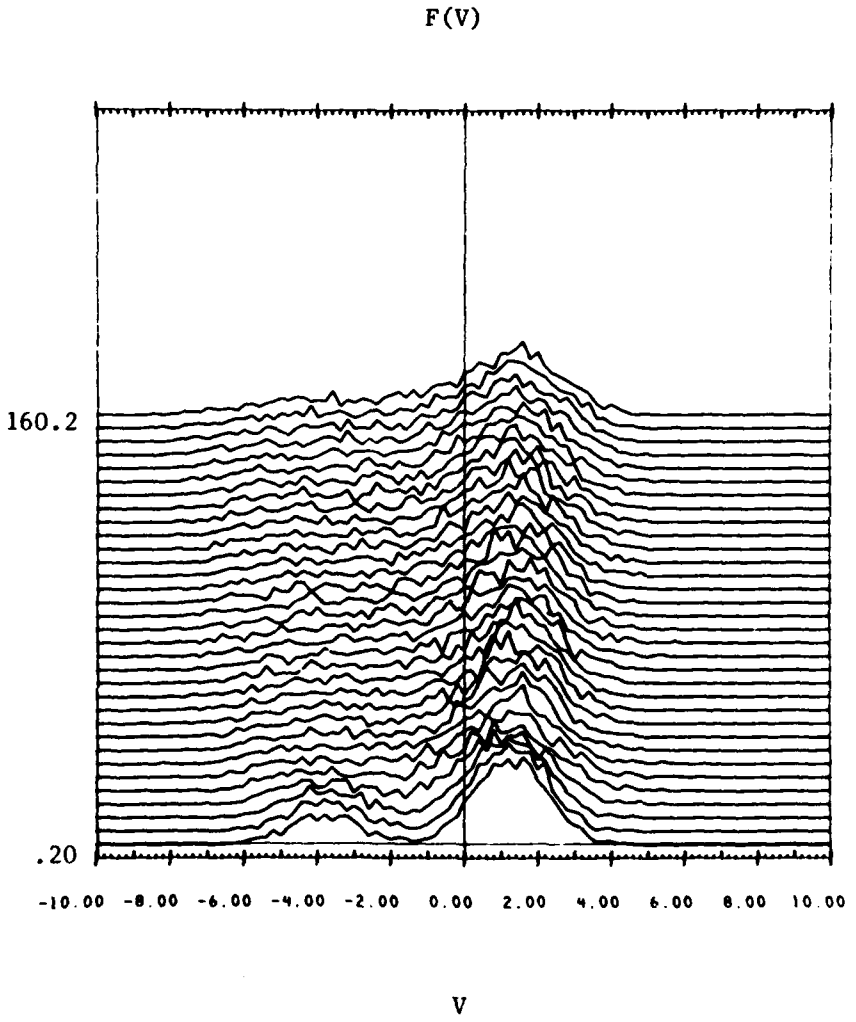

Figure 15. Histogram of the ion distribution function for a simulation where the initial distribution is being replenished.

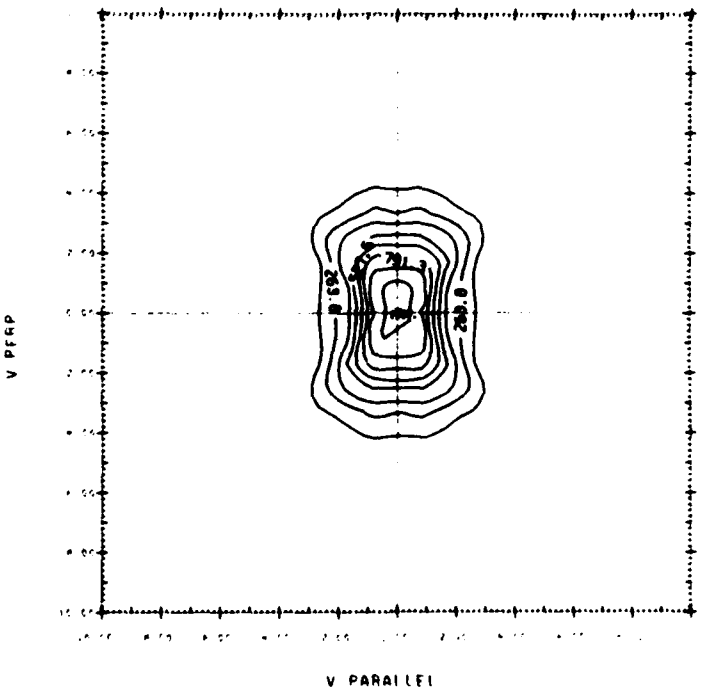

Figure 16. The initial ion loss cone distribution for the 2 1/2-D runs. A mirror ratio of two was assumed. This provided a velocity peak at approximately 2 $\times 10^8$ cm/sec.

$$f(v_\perp^2, v_\parallel) = \frac{\alpha_\perp \alpha_\parallel^{1/2}}{\pi^{3/2}} \left(\frac{R}{R-1}\right) e^{-(\alpha_\parallel v_\parallel^2)} \left(e^{-(\alpha_\perp v_\perp^2)} - e^{(\alpha_\perp R v_\perp^2)}\right)$$

where R is the mirror ratio, $\alpha = m/2kT$, and T is the parallel or perpendicular temperature.

The choice of temperature and mirror ratio were made to be consistent with the energy available to the counterstreaming ions in the Starfish case. Here we attempted to emulate a loss cone distribution in perpendicular velocity space that had a peak in it at about 1 to 2 $\times 10^8$ cm/sec where the fact that the ions in the simulation are light was considered.

As discussed earlier, it was decided after testing that using $\Delta z = 40\ \lambda_{De}$ would be stable and with appropriate use of the splines finite grid effects common to such large cell sizes would be overcome. This was confirmed in tests where we detected no spurious heating of the particles, particularly the electrons, energy did not build up in the shortest parallel wavelength modes and we conserved energy to the same accuracy as the 1-D simulations, $(E - E_o)/E \sim 10^{-4}$.

The evolution of the loss cone distribution can be seen in Figures 16-18 where the contours along the $v_\perp = 0$ line are seen to expand outward smoothing the contours. As expected from quasilinear theory the loss-cone fills in the depletion in $v_\parallel$ space but it does not appear to diffuse to high energy in $v_\perp$ space as the 1-D beam case did. At the time shown in Figure 18 the process is not complete but there is no evidence to suggest that nonlinear diffusion in the

perpendicular velocity space will occur to any appreciable extent at this late time in the simulation.

The electric field behavior was very interesting. The total electric field energy in the system saturated at approximately 7×10^{-3} of the thermal energy. This was a factor of at least ten less than the one dimensional simulation with the same number of particles per cell, 8, but no extra drift velocity energy available to the system. There was a very definite $k_{||}$ dependence to the perpendicular electric field, $E_{k_\perp}$. The parallel electric field, $E_{k_{||}}$, demonstrated both a $k_\perp$ and $k_{||}$ dependence but eventually the mode with the most energy was one where $\lambda_\perp = \lambda_{||}$. It was also noted that the peak parallel potential, $\phi_{||}$, was approximately one half of the perpendicular peak, $\phi_\perp$ for different modes. They did not peak at the same time. Figures 19 and 20 are representative of the type of dependences that were found.

The mode that grows earliest is one where $\lambda_\perp/\lambda_{||} \sim 1/40$ consistent with most analytical work. As the simulation progresses, the energy in the perpendicular electric field cascades into the flute mode where $k_{||} = 0$. Ultimately the preponderance of energy is spread among modes having one of four available parallel components. Figures 21, 22, and 23 show the temporal variations in the whole electric field spectrum. There is little doubt that some nonlinear wave-wave coupling is occurring but not to the extent seen in the one-dimensional simulations. As can be seen by comparing $e\phi/kT$ for both sets of simulations, Figures (8 and 19) the 2 1/2-D runs produced much lower levels of potential fluctuation per mode.

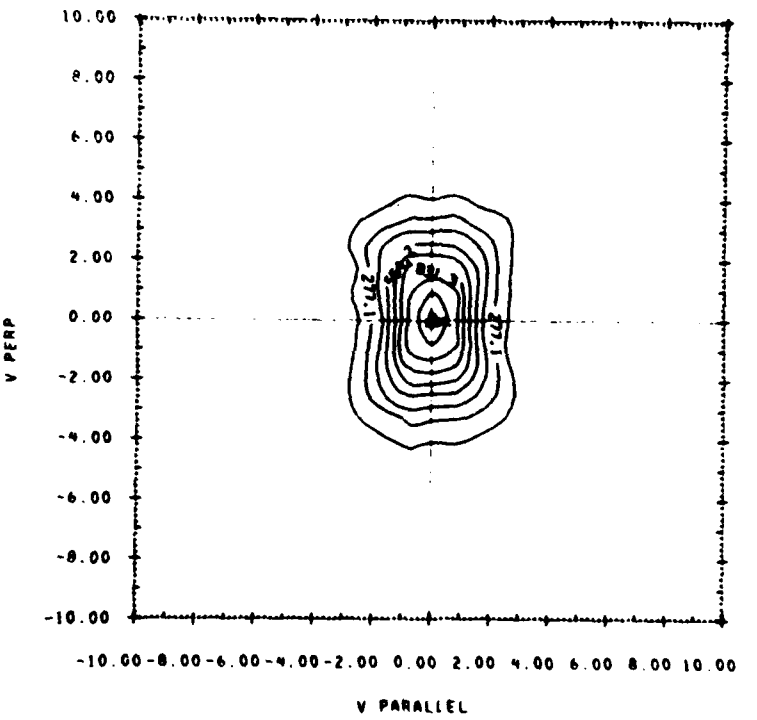

Figure 17. The ion loss cone distribution at $t \sim 80/\omega_{pe}$.

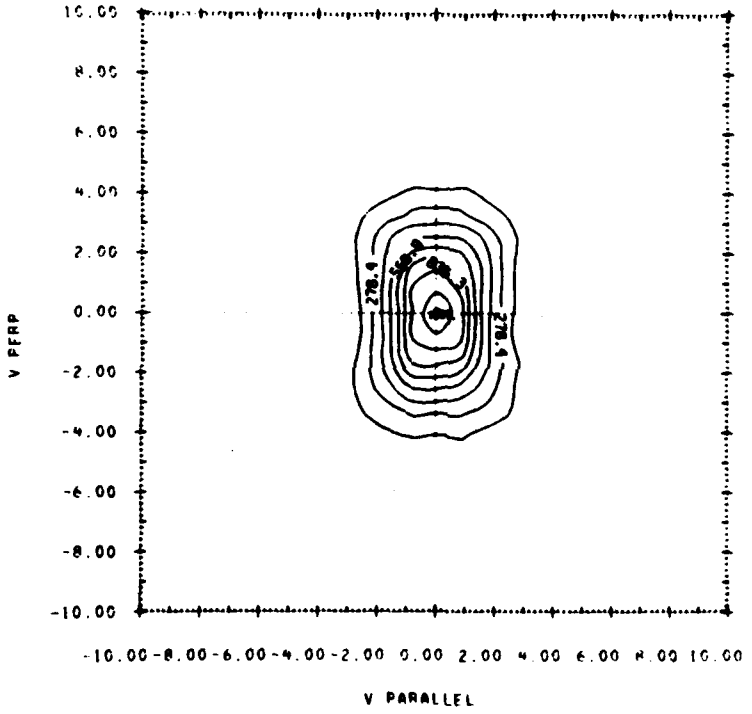

Figure 18. The ion loss cone distribution at the end of the simulation, $t = 160/\omega_{pe}$.

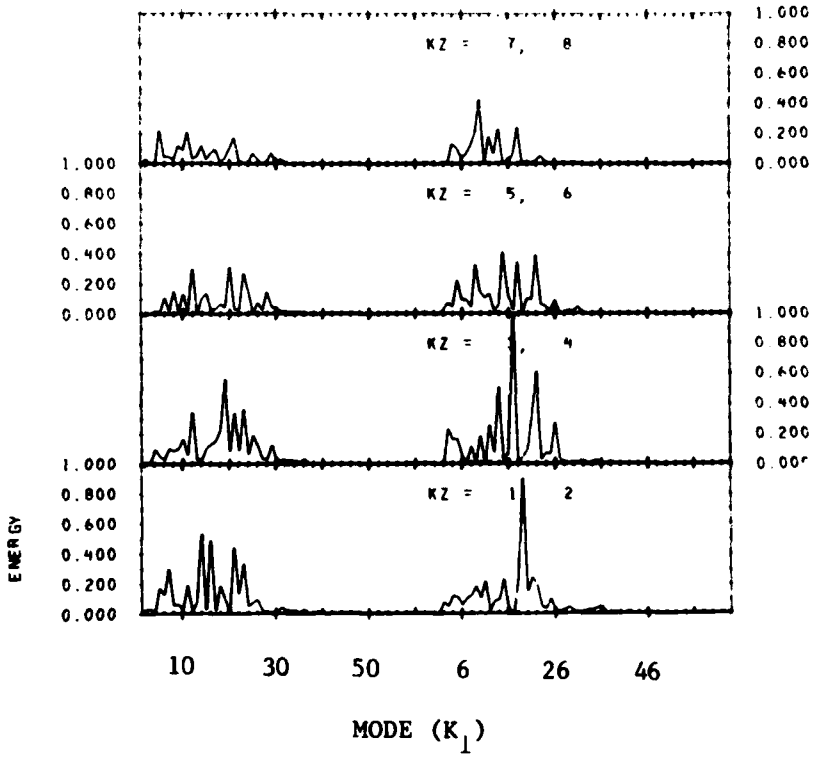

Figure 19. Shown here is the mode spectrum for the perpendicular electric field energy. All of the $k_\perp$ spectrum is shown for $k_{||}$ ranging from one to eight. The maximum $e\phi/kT$ shown here is 9.4×10^{-5}. Two sets of $k_\perp$ data are plotted on each ordinate axis ranging from 1 to 64 and then repeated.

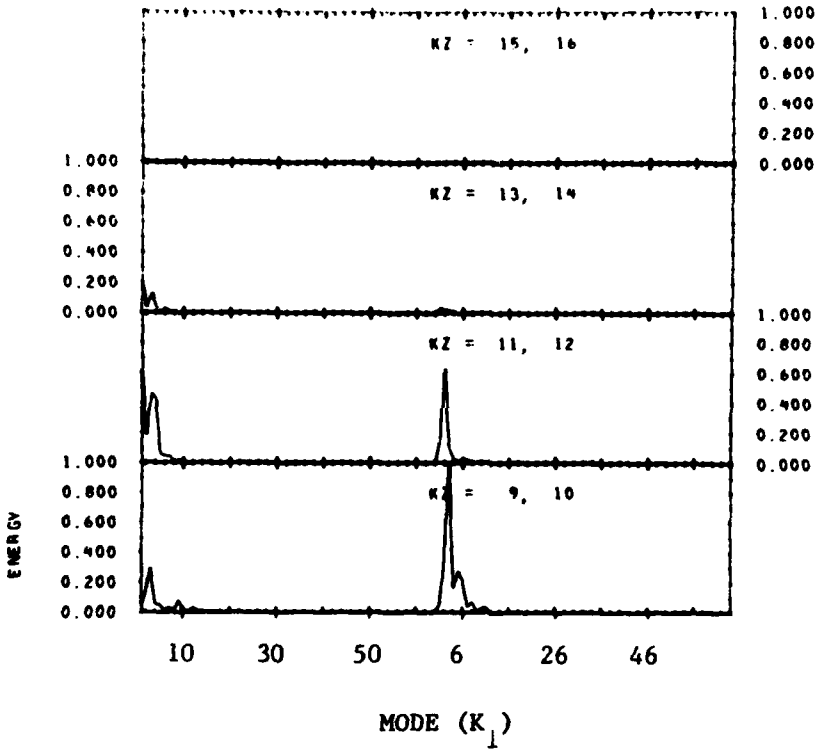

Figure 20. Shown here is a part of the parallel electric field energy spectrum. All of the $k_{\perp}$ spectrum is displayed for $k_{\parallel}$ ranging from nine to sixteen. The maximum $e\phi/kT$ in this plot is 1.5×10^{-5}. Two sets of $k_{\perp}$ data are plotted on each ordinate axis ranging from 1 to 64 and then repeated.

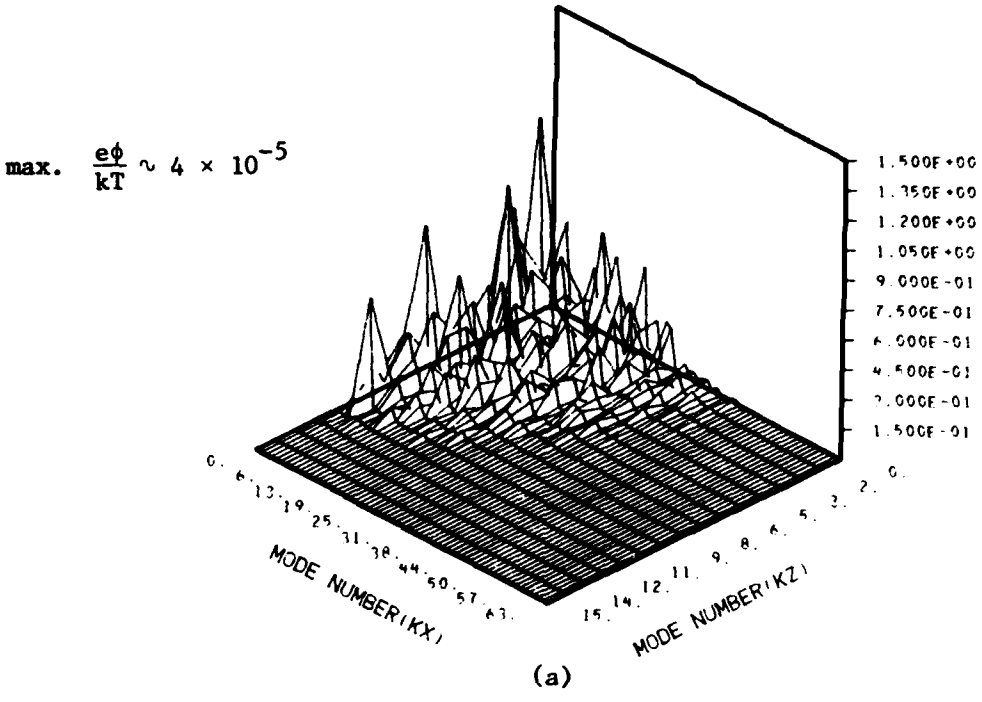

(a)

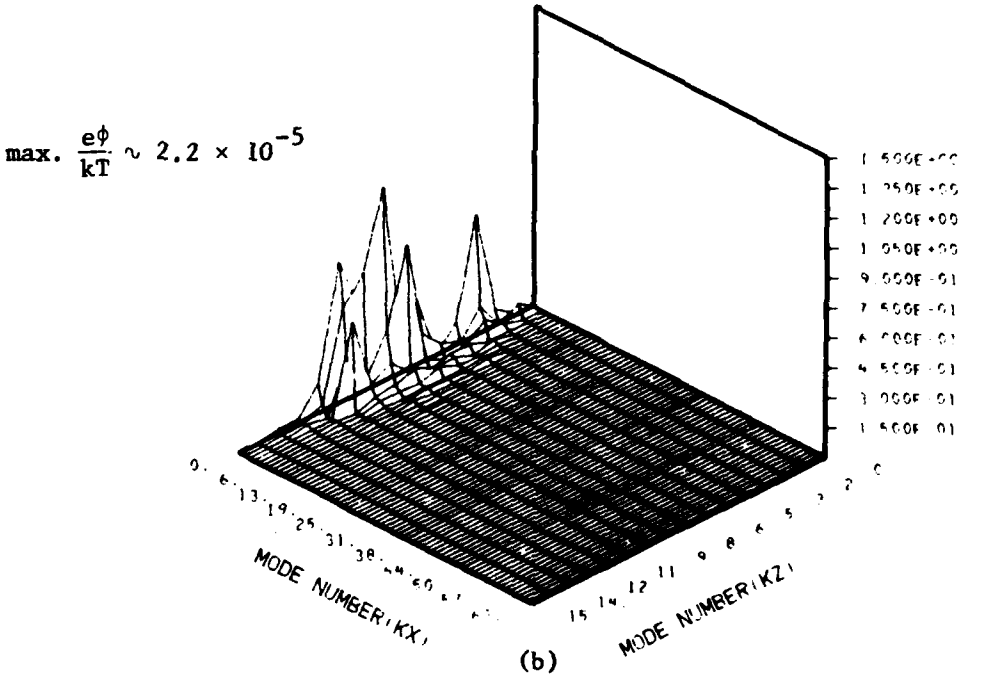

(b)

Figure 21. Perspective plots of the electric field energy at $t = 9.2/\omega_{pe}$, after the initial linear growth of the instabilities. (a) The perpendicular field energy. (b) The parallel field energy.

max. $\frac{e\phi}{kT} \sim 9.8 \times 10^{-5}$

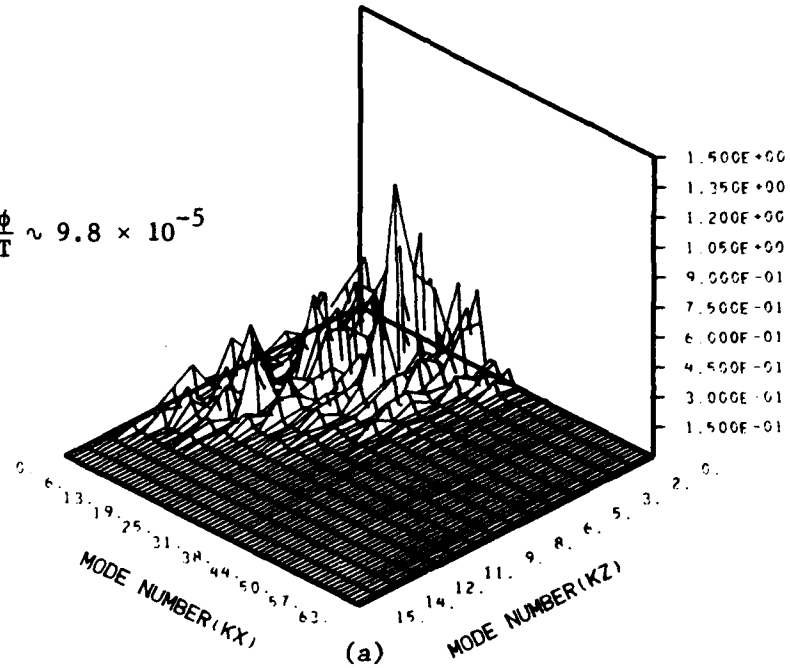

(a)

max. $\frac{e\phi}{kT} \sim 3.0 \times 10^{-5}$

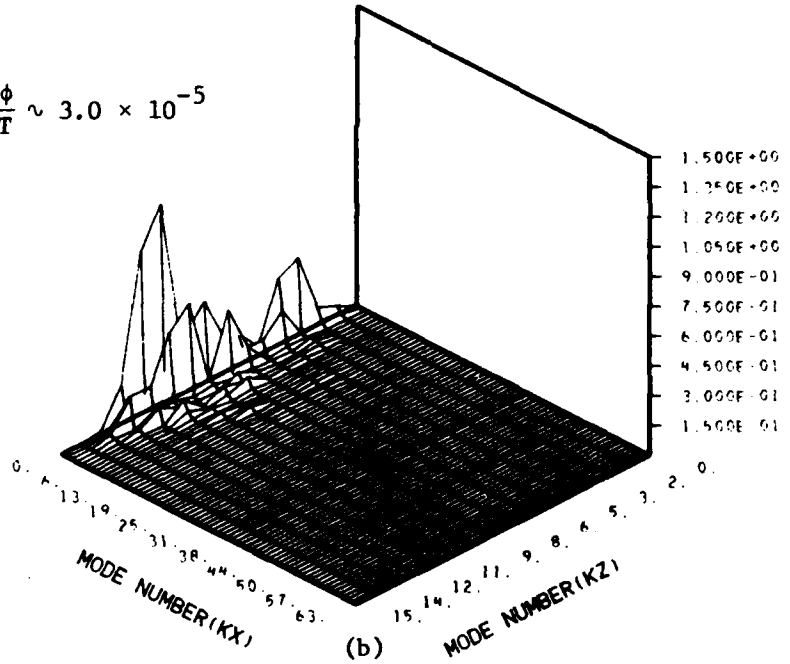

(b)

Figure 22. The electric field energy at $t = 80.2/\omega_{pe}$. Figures 21-23 are all self normalized comparison can only be made by noting the maximum amplitude on each plot. (a) The perpendicular field energy. (b) The parallel field energy.

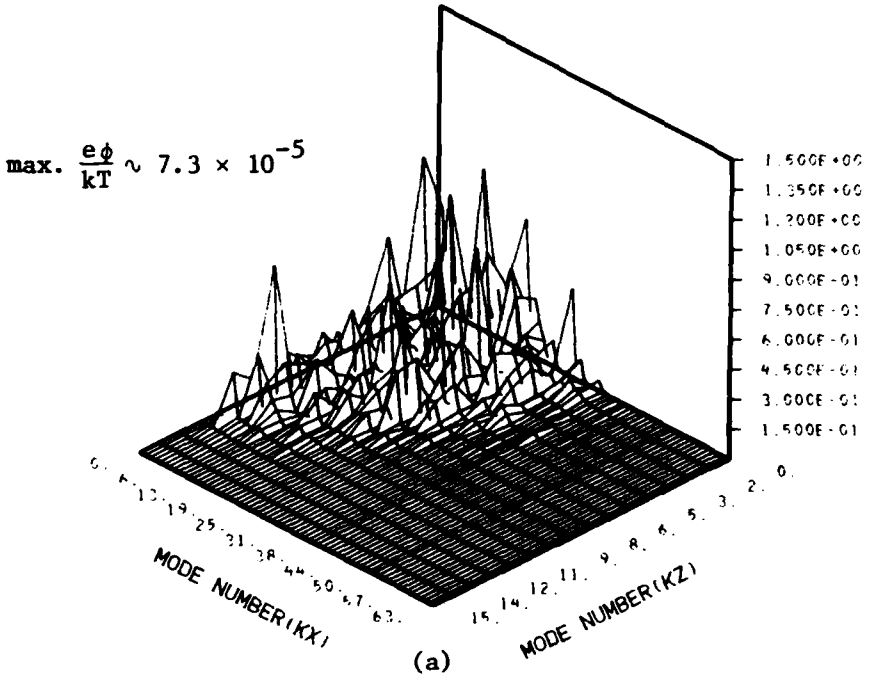

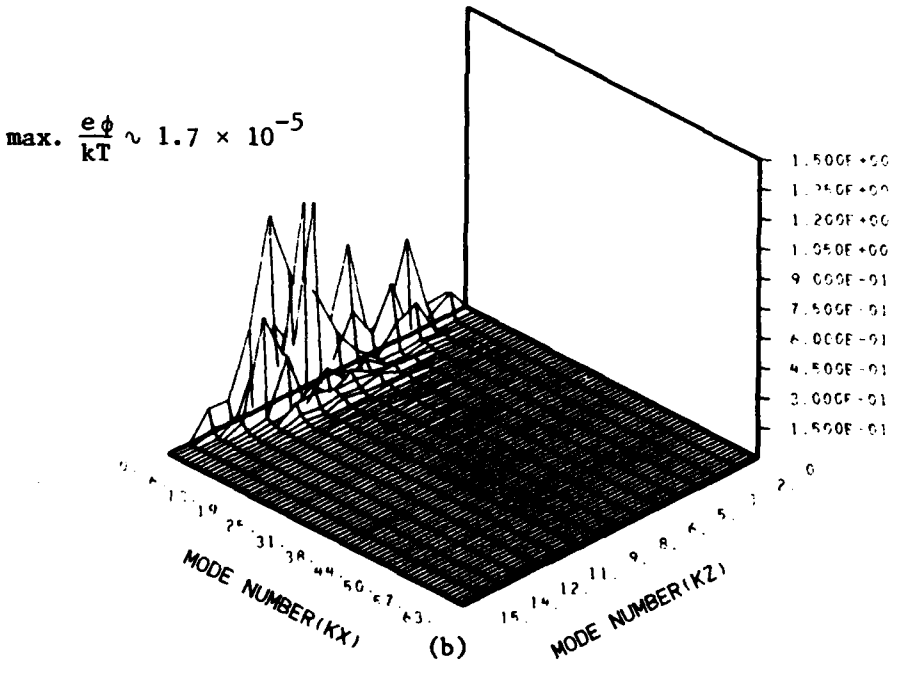

Figure 23. The same data as Figures 21 and 22 shown at $t = 160.2/\omega_{pe}$.

The frequency for the largest amplitude mode in the system, $k = (k_{||}, k_{\perp}) = (4,17)$, should from equation (3) be $\omega \sim \frac{1}{40}\omega_{pe} \sim .03\ \omega_{pe}$. Estimates from the simulations, Figure 24, produce $\gamma \sim .11\ \omega_{pe}$ and $\omega \sim .04\omega_{pe}$ considering finite particle width effects of dispersion relations. Using $e\phi/kT$, the wavelength of the modes and a $\Delta v_{\perp}^2 \sim (v_{thi}/4)^2$ one can estimate the quasilinear diffusion time from Eq. 6. The result is that $\tau_q \sim 56/\omega_{pi}$. This agrees with our result reasonably well, Figures 16 and 17.

The 2-D simulation was performed with a replenishment algorithm in it. Here we replenished at the rate of 10 particles randomly throughout the distribution. One can estimate what the particle flux into a simulation region such as used here would be in the H.A.N.E. case. For the estimate I chose $v \sim 1 \times 10^8$ cm/sec and $n_o \sim 7 \times 10^8$ particle/cm^3. This resulted in a flux into the grid of 0.22 particles/ω_{pe} where for the simulation $\Delta t = .2/\omega_{pe}$. Because of the attempt by the algorithm to maintain the original distribution we feel that the effect of incoming plasma to the interaction region is more than adequately modeled here.

In summary we have begun research into possible field aligned acceleration. One dimensional simulations were performed using beams of unequal density. This is throught to be the case for regions of the interactions in the H.A.N.E. It was found that large potentials were generated in very discrete modes. Strong diffusion was produced in a fashion consistent with theory and earlier simulations for counterstreaming plasmas. The less dense of the two beams experienced energy diffusion both up and

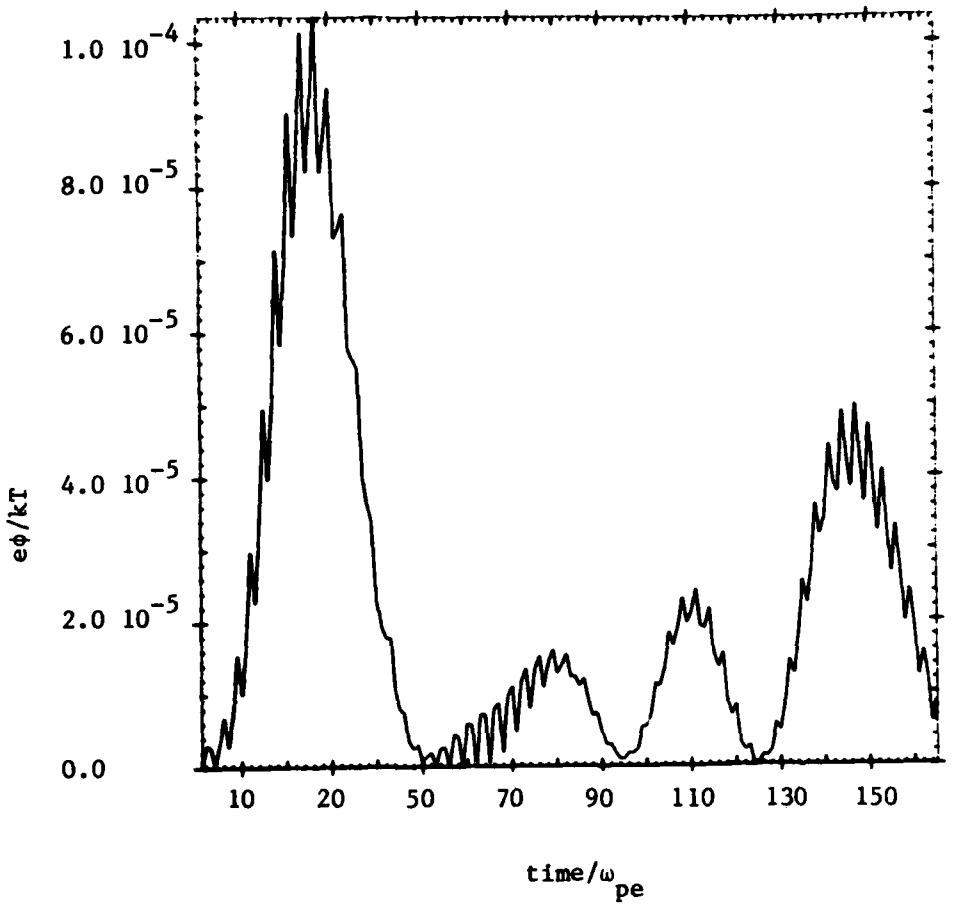

Figure 24. The amplitude of the mode, $k_{||} = 4$, $k_{\perp} = 17$, as a function of time.

down the energy spectrum while the dense beam experienced a small amount of high energy diffusion. The diffusion was very fast, occurring on the time scale of twenty electron plasma periods. In the two dimensional simulations a true loss cone simulation was undertaken. The electric field energy was found to be considerably lower than for the 1-D simulation. In addition the energy in the perpendicular electric field was shared by many modes and had a $k_{\parallel}$ dependence. A parallel electric field was produced. The maximum potential found in a parallel mode was approximately one half of the maximum potential found in a perpendicular mode. The level of maximum potential for any given mode was orders of magnitude below that found in the 1-D case. As expected the loss cone filled but little diffusion to high energy was noted in the perpendicular portion of the distribution.

In the next section a discussion of the implications of these results and the questions they raise will be presented. In addition ideas about future directions will also be presented.

SECTION V

CONCLUSIONS

The results discussed in this report are a preliminary attempt to understand the mechanisms that cause field aligned accelerations in a H.A.N.E. The 1-D and 2 1/2-D codes were found to agree well with known quasilinear and nonlinear theory where checks were possible. It was found in this reasearch that the standard loss cone distribution represented by a thermalized unmagnetized ion plasma with a hole in parallel velocity space does not provide the scattering parallel to the magnetic field which was predicted by Clark and Papadopoulos.[1] In the 2 1/2-D runs diffusion did fill the loss cone but did not generate the fluctuations necessary for diffusion to high energy. It appears from comparing the 1-D results with the 2 1/2-D results that in a thermalized loss cone not enough free energy is available to produce sufficiently large potential fluctuations. This implies that the traditional or standard loss cone instability produced by a simple hole in a thermalized ion distribution will not be energetic enough to produce a hard spectrum with velocities comparable or above the expansion velocity.

These results do not rule out the explanation put forward by Clark and Papadopoulos but do require that their explanation be more broadly interpreted. As mentioned in Section III, there is a broader interpretation and use of the term loss cone. The term loss cone instability has been applied to beam plasma type instabilities where no particle loss mechanism exists.

In this light, there is still the possibility that a loss cone type instability might explain the high energy spectrum detected in the Southern Conjugate.[11,12] A more appropriate description would be a beam plasma instability of which there are several possible. Recall from Figure 3 that the less dense plasma distribution was diffused to energies $\sim$ 50% above its mean energy. Recall also that at 15 keV an oxygen atom has only 3×10^7 cm/sec velocity while the streaming velocity is on order $1\text{-}2 \times 10^8$. From the evolution of the 2-D contour plots, it is conceivable that isotropization of the distorted beam into parallel space could produce the spectrum predicted if one allows for higher perpendicular energy at the outset. This possiblility will be examined in the near future. In addition the inverse mirror geometry of the magnetic field will also be considered as a possible acceleration mechanism. Here the ions must be magnetized.

There are several differences between this research and some of the theory used to describe the loss cone instability. The major one occurs because a symmetry perpendicular to the magnetic field is assumed in most analyses. However, in the 2 1/2-D simulations such a symmetry does not exist. The particles can gyrate in the third velocity but they cannot generate a wave spectrum or damp modes in that spatial dimension. This prevents damping of modes through the relation, $\omega = v_\perp k_\perp \cos\theta$ where θ is the angle in the perpendicular plane. Such damping could conceivably produce more heating. However, if scattering caused by large potential fluctuations is the major phenomena to be investigated such damping would only inhibit the scattering. An

example of such scattering although caused by numerics is seen in Figure 1.

In the H.A.N.E. case such symmetries are not likely at the early times when the plasma has its maximum streaming energy. As shown in the 1-D simulations, diffusion occurs on time scales of the ion plasma frequency. Using parameters typical of Starfish for oxygen and allowing for a modest amount of field compression, .84G, one gets that $\omega_{pe} \sim 10^8$, $\omega_{pi} \sim 5 \times 10^5$, $\omega_{ce} \sim 10^7$ and that $\omega_{ci} \sim 5 \times 10^2$, The three order of magnitude difference between the ion frequencies implies that if beaming instabilities do operate in the interaction region they will occur to the exclusion of magnetic behavior on the part of the ions. This result can be altered if the ions become highly ionized and/or the magnetic field is compressed by amounts approaching an order of magnitude. Both events are possible; in some simulations[6,18] magnetic compression of a factor of 20 have been produced. Because of the rapid diffusion one also has to consider the ability of the interaction region to maintain a loss cone. As was seen in the replenishment simulations, the rate plasma will stream into this region will be slower than the diffusion rate. This implies that spatial effects may become very important and that the scattering mechanism may not be steady state. The possibility of sporadic coupling is suggested by the behavior of modes as seen in Figures 10 and 24. The upshot of this could be the production of structure in deposition and the expanding debris.

An additional difference between this research and the standard analytic theory is that typically it is assumed that the real frequency, ω_r, is greater than the growth

rate, γ. Often this is an assumption of mathematical convenience particularly for high frequency modes. Our simulations typically find $\gamma \geq \omega_r$ at least at the beginning of the simulation. As the simulation continues this relation relaxes and $\gamma \leq \omega_r$ is noted.

A possible deficiency in the results shown was the lack of duration for the simulation. The simulations were only run out to $160/\omega_{pe}$. It was felt however that in the preliminary phase of this research that we were looking for tendencies of the plasma to be scattered down the field line. If such tendencies were seen in any of the runs made, we were prepared to carry the run out. However, in all cases the dynamics and sources of free energy had been diffused by the instabilities to levels that appeared to offer small chance of scattering. In the two dimensional case none of the runs showed any appreciable electron heating attesting to the low level of fluctuation. In the parallel direction the wavelength had been selected to miss the electron Landau damping region. In perpendicular space the electron distribution function and its moments changed little.

There is an important question that must be addressed. And that is the question of timing. If the scattering is occurring as a direct result of electrostatic instabilities the effect of the magnetic field may be minimal. As seen in Figures 3 and 4 only a small fraction of the plasma was diffused to high energy but it carried most of the energy flux in the center of mass frame. The small density distribution was heavily diffused while the massive one was not. If the beams had been of equal mass each beam would be diffused but not to as high an energy. This is because the center of mass

velocity of either beam relative to the thermal velocity would have been lower. If the scattering persists or occurs for time greater than ω_{ci} then the magnetic field, its gradient and such may play a prominant role because a high beta situation exists. It then becomes necessary to look into the effects of Whistlers and other electromagnetic phenomena as a means of scattering. In this case the plasma one might be dealing with would be a thermalized or heavily diffused ion distribution that is anisotropic, nonmaxwellian and might encompass most of the plasma in the interaction region. In addition one could be forced to consider the loss down the field line because at these times parallel transport must be considered. In short, it appears that the question of timing is crucial to the determination of whether part or most of the plasma in the interaction region is involved in the dynamics of field aligned scattering.

In summary we feel that several questions have been answered by this work and that the principal questions remain to be answered. Our work indicates that the standard loss cone will not be energetic enough to provide the speculated high energy spectrum. The one dimensional simulations reaffirmed the rapid diffusion that can be expected from energetic beam-plasma interaction. Questions remain as to whether or not the diffusion seen in the 1-D simulation will persist in 2 1/2-D and whether or not plasma can be sent down the magnetic field lines. Timing becomes important here because it will determine the role played by the magnetic field. We suggest that timing may also determine the shape of the spectrum and the amount of energy and plasma coming down the field line.

A possible scenario for an energetic parallel spectrum to occur is the interaction of two relatively cold beams which produce the kind of diffusion upward in energy seen in the one dimensional code. If this high energy plasma is then diffused parallel by electromagnetic effects such as ion whistlers[17] then one could conceivably end up with a very energetic parallel spectrum.

Our future research is directed toward answering these questions. A mix of electrostatic and electromagnetic simulations will be undertaken to consider these problems and resolve them.

REFERENCES

1. Clark, R.W. and K. Papadopoulos, "A model for the computation of debris patches after a H.A.N.E. (Appl. to Starfish)," UNPUBLISHED.

2. Post, R.F. and M.N. Rosenbluth, "Electrostatic instabilities in finite mirror-confined plasmas," Phys. Fluids, 9, 730, (1966).

3. Palmadesso, P.J., Primate Communication, NRL, Sept. (1979).

4. Longmire, C.L., R.W. Kilb, and W.F. Crevier, "The CMHD approach to high altitude blast waves," DNA 3313T, July (1974).

5. Kilb, R.W. and D.E. Glenn, "CMHD simulations of very high altitude nuclear bursts from 0 to 1 sec.," UNPUBLISHED.

6. Clark, R.W., J. Denavit and K. Papadopoulos, "Laminar interactions in high mach number plasma flows," Phys. Fluids, 16, 1097, (1973).

7. Clark, R.W., T. Coffey and K. Papadopoulos, "Numerical simulation of coupling in Starfish," UNPUBLISHED.

8. Gerver, M.J., "Critical lengths for high density mirror machines," Phys. Fluids, 23, 755, (1980).

9. Cohen, B.I. and N. Maron, "Some nonlinear properties of drift-cone modes," Phys. Fluids, 23, 974, (1980).

   Cohen, B.I., N. Maron, and G.R. Smith, "Some nonlinear properties of drift-cyclotron modes," Phys. Fluids, 25, 826, (1982).

10. Hitchcock, D.A., S.H. Brecht, and W. Horton, Jr., "The neutral beam driven convective loss cone instability in torodial geometry," Phys. Fluids, 20, 1551, (1977).

11. Brecht, S.H. and P.J. Palmadesso, "Quasilinear scattering from waves driven by beam-plasma instabilities," NRL Memo Report #4203, (1980).

12. Brecht, S.H., R. Clark, P.J. Palmadesso, and E. Hyman, "The Starfish southern conjugate rebrightening," UNPUBLISHED.

13. Davidson, R.C., Methods in Nonlinear Plasma Theory, Academic Press, New York, NY, 1972.

14. Galeev, A.A., "Ion escape from a magnetic mirror trap due to development of instability connected with the 'loss cone'," Soviet Phys. JETP, 22, 466, (1966).

15. Galeev, A.A., "Quasilinear theory of the loss-cone instability," J. Plasma Phys., 1, part 1, 105, (1967).

16. Anderson, N., "On the calculation of filter coefficients for maximum entropy spectral analysis," Geophys., 29, 69, (1974).

17. Sagdeev, R.Z. and A.A. Galeev, Nonlinear Plasma Theory, W.A. Benjamin, New York, NU, 1969.

18. Clark, R.W., Private communication on KLYSMA data.

DISTRIBUTION LIST

DEPARTMENT OF DEFENSE

Assistant to the Secretary of Defense
Atomic Energy
ATTN: Executive Assistant

Command & Control Tech Ctr
ATTN: C-650, G. Jones
ATTN: C-650
ATTN: C-312, R. Mason
3 cy ATTN: C-650, W. Heidig

Defense Advanced Rsch Proj Agency
ATTN: GSD, R. Alewene
ATTN: STO, W. Kurowski

Defense Comm Agency
ATTN: Code 205
ATTN: Code 230
ATTN: J300 for Yen-Sun Fu

Defense Comm Engineer Ctr
ATTN: Code R123
ATTN: Code R410, N. Jones
ATTN: Code R410

Defense Intelligence Agency
ATTN: DB, A. Wise
ATTN: DB-4C
ATTN: DT-1B
ATTN: Dir
ATTN: DC-7B

Defense Nuclear Agency
ATTN: NATD
ATTN: RAEE
ATTN: STNA
ATTN: RAAE, P. Lunn
ATTN: NAFD
3 cy ATTN: RAAE
4 cy ATTN: TITL

Defense Tech Info Ctr
12 cy ATTN: DD

Deputy Under Secretary of Defense
Comm, Cmd, Cont & Intell
ATTN: Dir of Intelligence System

Field Command
Defence Nuclear Agency, Det 1
Lawrence Livermore National Lab
ATTN: FC-1

Field Command
Defense Nuclear Agency
ATTN: FCPR
ATTN: FCTXE
ATTN: FCTT, G. Ganong
ATTN: FCTT, W. Summa

Interservice Nuclear Weapons School
ATTN: TTV

Joint Chiefs of Staff
ATTN: C3S
ATTN: C3S, Evaluation Office, HDOO

DEPARTMENT OF DEFENSE (Continued)

Joint Strat Tgt Planning Staff
ATTN: JPPFD
ATTN: JPTM
ATTN: JLAA
ATTN: JPSS
ATTN: JLKS
ATTN: JLK, DNA Rep

National Security Agency
ATTN: W-32, O. Bartlett
ATTN: B-3, F. Leaonard

Under Secretary of Defense for Rsch & Engrg
ATTN: Strat & Theater Nuc Forces, B. Stephan
ATTN: Strategic & Space Sys (OS)

WWMCCS System Engrg Org
ATTN: J. Hoff

DEPARTMENT OF THE ARMY

Army Logistics Management Ctr
ATTN: DLSIE

Assistant Chief of Staff for Automation & Comm
ATTN: DAMO-C4, P. Kenny

Atmospheric Sciences Lab
ATTN: DELAS-EO, F. Niles

BMD Advanced Technology Ctr
ATTN: ATC-R, W. Dickinson
ATTN: ATC-R, D. Russ
ATTN: ATC-T, M. Capps
ATTN: ATC-O, W. Davies

BMD SYstems Cmd
ATTN: BMDSC-HLE, R. Webb
2 cy ATTN: BMDSC-HW

Deputy Chief of Staff for Ops & Plans
ATTN: DAMO-RQC, C2 Div

Harry Diamond Labs
ATTN: DELHD-NW-R, R. Williams
2 cy ATTN: DELHD-NW-P

US Army Chemical School
ATTN: ATZN-CM-CS

US Army Comm-Elec Instal Agency
ATTN: CCC-CED-CCO, W. Neuendorf
ATTN: CCC-EMEC-PED, G. Lane

US Army Comm Cmd
ATTN: CC-OPS-W
ATTN: CC-OPS-WR, H. Wilson

US Army Comm R&D Cmd
ATTN: DRDCO-COM-RY, W. Kesselman

US Army Foreign Science & Tech Ctr
ATTN: DRXST-SD

US Army Nuclear & Chemical Agency
ATTN: Library

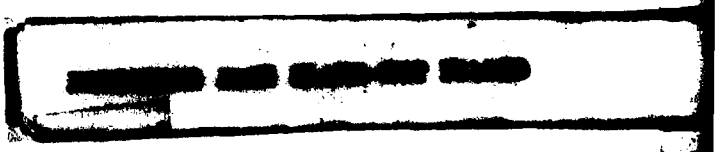

DEPARTMENT OF THE ARMY (Continued)

US Army Materiel Dev & Readiness Cmd
ATTN: DRCLDC, J. Bender

US Army Satellite Comm Agency
ATTN: Doc Con

US Army TRADOC Sys Analysis Actvy
ATTN: ATAA-TDC
ATTN: ATAA-PL
ATTN: ATAA-TCC, F. Fayan, Jr

US Army White Sands Missile Range
ATTN: STEWS-TN-N, K. Cummings

USA Missile Cmd
ATTN: DRSMI-YSO, J. Gamble

DEPARTMENT OF THE NAVY

Joint Cruise Missiles Project Office
ATTN: JCMG-707

Naval Air Systems Cmd
ATTN: PMA 271

Naval Electronic Systems Cmd
ATTN: PME 106, F. Diederich
ATTN: PME 117-211, B. Kruger
ATTN: PME 106-4, S. Kearney
ATTN: Code 3101, T. Hughes
ATTN: Code 501A
ATTN: PME 117-2013, G. Burnhart
ATTN: PME 106-13, T. Griffin
ATTN: PME 117-20

Naval Intelligence Support Ctr
ATTN: NISC-50

Naval Ocean Systems Ctr
ATTN: Code 532
ATTN: Code 5322, M. Paulson
ATTN: Code 5323, J. Ferguson

Naval Rsch Lab
ATTN: Code 4780, S. Ossakow
ATTN: Code 4108, E. Szuszewicz
ATTN: Code 4720, J. Davis
ATTN: Code 6700
ATTN: Code 7950, J. Goodman
ATTN: Code 4780
ATTN: Code 4187
ATTN: Code 7500, B. Wald
ATTN: Code 4700

Naval Space Surveillance System
ATTN: J. Burton

Naval Surface Weapons Ctr
ATTN: Code F31

Naval Telecommunications Cmd
ATTN: Code 341

DEPARTMENT OF THE NAVY (Continued)

Ofc of the Deputy Chief of Naval Ops
ATTN: NOP 941D
ATTN: NOP 981N
ATTN: NOP 654, Strat Eval & Anal Br

Office of Naval Rsch
ATTN: Code 414, G. Joiner
ATTN: Code 412, W. Condell

Strategic Systems Project Office
ATTN: NSP-43
ATTN: NSP-2141
ATTN: NSP-2722

Theater Nuclear Warfare Prj Office
ATTN: PM-23, D. Smith

DEPARTMENT OF THE AIR FORCE

Air Force Geophysics Lab
ATTN: LYD, K. Champion
ATTN: OPR-1
ATTN: R. Babcock
ATTN: CA, A. Stair
ATTN: OPR, H. Gardiner
ATTN: PHY, J. Buchau
ATTN: R. O'Neil

Air Force Satellite Ctrl Facility
ATTN: WE

Air Force Space Technology Ctr
ATTN: YH

Air Force Tech Applications Ctr
ATTN: TN

Air Force Weapons Lab
ATTN: SUL
ATTN: NTN

Air Force Wright Aeronautical Lab
ATTN: A. Johnson
ATTN: W. Hunt

Air Logistics Cmd
ATTN: OO-ALC-MM

Air University Library
ATTN: AUL-LSE

Assistant Chief of Staff
Studies & Analysis
ATTN: AF/SASC, C. Rightmeyer

Ballistic Missile Office
ATTN: ENSN, W. Wilson
ATTN: ENSN
ATTN: SYC, D. Kwan

DEPARTMENT OF THE AIR FORCE (Continued)

Deputy Chief of Staff
Rsch, Dev, & Acq
ATTN: AFRDQI
ATTN: AFRDS, Space Systems & C3 Dir

Deputy Chief of Staff
Plans and Operations
ATTN: AFXOKT
ATTN: AFXOKCD
ATTN: AFXOKS

Headquarters
Electronics Sys
ATTN: ESD/SCTE, J. Clark
ATTN: SCS-1E
ATTN: SCS-2, G. Vinkels

Foreign Technology Div
ATTN: TQTD, B. Ballard
ATTN: NIIS, Library

Rome Air Dev Ctr
ATTN: OCS, V. Coyne
ATTN: OCSA, R. Schneible
ATTN: TSLD
ATTN: EEP, J. Rasmussen
ATTN: EEPS, P. Kossey

Headquarters
Space Command
ATTN: DC, T. Long

Strategic Air Command
ATTN: ADWA
ATTN: XPQ
ATTN: XPFC
ATTN: DCXN
ATTN: DCZ
ATTN: NRI-STINFO, Library
ATTN: XPFS

DEPARTMENT OF ENERGY

Department of Energy
GTN
ATTN: DP-233

OTHER GOVERNMENT AGENCIES

Central Intelligence Agency
ATTN: OSWR/NED
ATTN: OSWR/SSD for K. Feuerpfetl

Department of Commerce
National Bureau of Standards
ATTN: Sec Ofc for R. Moore

Department of Commerce
National Oceanic & Atmospheric Admin
ATTN: R. Grube

Department of State
Office of International Security Policy
ATTN: PM/STM

OTHER GOVERNMENT AGENCIES (Continued)

Institute for Telecommunications Sciences
ATTN: A. Jean
ATTN: L. Berry
ATTN: W. Utlaut

DEPARTMENT OF ENERGY CONTRACTORS

EG&G, Inc
Attention Document Control for
ATTN: D. Wright
ATTN: J. Colvin

University of California
Lawrence Livermore National Lab
ATTN: L-31, R. Hager
ATTN: Tech Info Dept, Library

Los Alamos National Lab
ATTN: MS 670, J. Hopkins
ATTN: P. Keaton
ATTN: D. Simons
ATTN: MS 664, J. Zinn
ATTN: T. Kunkle, ESS-5
ATTN: J. Wolcott
ATTN: R. Jeffries

Sandia National Labs
ATTN: T. Cook
ATTN: B. Murphey

Sandia National Labs
ATTN: Tech Lib, 3141
ATTN: Org 1250, W. Brown
ATTN: Org 4231, T. Wright
ATTN: D. Thornbrough
ATTN: Space Project Div
ATTN: D. Dahlgren

DEPARTMENT OF DEFENSE CONTRACTORS

Aerospace Corp
ATTN: D. Olsen
ATTN: I. Garfunkel
ATTN: J. Ailey
ATTN: J. Kluck
ATTN: D. Whelan
ATTN: R. Slaughter
ATTN: J. Straus
ATTN: K. Cho
ATTN: V. Josephson
ATTN: T. Salmi

Aerospace Corp
ATTN: S. Mewaters

Analytical Systems Engrg Corp
ATTN: Radio Sciences

Analytical Systems Engrg Corp
ATTN: Security

BDM Corp
ATTN: T. Neighbors
ATTN: L. Jacobs

DEPARTMENT OF DEFENSE CONTRACTORS (Continued)

Berkeley Rsch Associates, Inc
ATTN: J. Workman
ATTN: C. Prettie
2 cy ATTN: S. Brecht
2 cy ATTN: J. Orens

Boeing Aerospace Co
ATTN: MS/87-63, D. Clauson

Boeing Co
ATTN: G. Hall
ATTN: S. Tashird

BR Communications
ATTN: J. McLaughlin

University of California at San Diego
ATTN: H. Booker

Charles Stark Draper Lab, Inc
ATTN: A. Tetewski
ATTN: D. Cox
ATTN: J. Gilmore

Computer Sciences Corp
ATTN: F. Eisenbarth

Comsat Labs
ATTN: D. Fang
ATTN: G. Hyde

Cornell University
ATTN: M. Kelly
ATTN: D. Farley, Jr

E-Systems, Inc
ATTN: R. Berezdivin

Electrospace Systems, Inc
ATTN: H. Logston
ATTN: P. Phillips

EOS Technologies, Inc
ATTN: W. Lelevier
ATTN: B. Gabbard

General Electric Co
ATTN: R. Juner
ATTN: A. Steinmeyer
ATTN: C. Zierdt

General Electric Co
ATTN: G. Millman

General Rsch Corp
ATTN: B. Bennett

Geo Ctrs, Inc
ATTN: E. Marram

GTE Communications Products Corp
ATTN: R. Steinhoff

DEPARTMENT OF DEFENSE CONTRACTORS (Continued)

GTE Communications Products Corp
ATTN: J. Concordia
ATTN: I. Kohlberg

Harris Corp
ATTN: E. Knick

Honeywell, Inc
ATTN: A. Kearns, MS924-3
ATTN: G. Terry, Avionics Dept

Horizons Technology, Inc
ATTN: R. Kruger

HSS, Inc
ATTN: D. Hansen

IBM Corp
ATTN: H. Ulander

Institute for Defense Analyses
ATTN: H. Gates
ATTN: J. Aein
ATTN: E. Bauer
ATTN: H. Wolfhard

International Tel & Telegraph Corp
ATTN: Tech Library

International Tel & Telegraph Corp
ATTN: G. Wetmore

JAYCOR
ATTN: J. Sperling

Johns Hopkins University
ATTN: C. Meng
ATTN: K. Potocki
ATTN: J. Phillips
ATTN: T. Evans
ATTN: J. Newland
ATTN: P. Komiske

Kaman Science Corp
ATTN: E. Conrad

Kaman Tempo
ATTN: DASIAC

Kaman Tempo
ATTN: DASIAC
ATTN: B. Gambill
ATTN: W. Schuleter
ATTN: W. McNamara

Litton Systems, Inc
ATTN: B. Zimmer

Lockheed Missiles & Space Co, Inc
ATTN: R. Sears
ATTN: J. Kumer

DEPARTMENT OF DEFENSE CONTRACTORS (Continued)

Lockheed Missiles & Space Co, Inc
ATTN: Dept 60-12
2 cy ATTN: D. Churchill, Dept 62-A1

M. I. T. Lincoln Lab
ATTN: V. Vitto
ATTN: D. Towle
ATTN: N. Doherty

MA/COM Linkabit Inc
ATTN: A. Viterbi
ATTN: I. Jacobs
ATTN: H. Van Trees

Magnavox Govt & Indus Electronics Co
ATTN: G. White

Maxim Technologies, Inc
ATTN: R. Morganstern
ATTN: E. Tsui
ATTN: J. Marshall

McDonnell Douglas Corp
ATTN: Tech Library Svcs
ATTN: W. Olson
ATTN: R. Halprin

Meteor Comms Corp
ATTN: R. Leader

Mission Research Corp
ATTN: G. McCartor
ATTN: D. Knepp
ATTN: R. Bogusch
ATTN: F. Guigliano
ATTN: F. Fajen
ATTN: Tech Library
ATTN: R. Bigoni
ATTN: R. Dana
ATTN: S. Gutsche
ATTN: R. Hendrick
ATTN: R. Kilb
4 cy ATTN: C. Lauer

Mitre Corp
ATTN: A. Kymmel
ATTN: C. Callahan
ATTN: G. Harding
ATTN: MS J104, M. Dresp

Mitre Corp
ATTN: W. Hall
ATTN: W. Foster
ATTN: M. Horrocks
ATTN: J. Wheeler

Pacific-Sierra Rsch Corp
ATTN: F. Thomas
ATTN: H. Brode, Chairman SAGE
ATTN: E. Field, Jr

Pennsylvania State University
ATTN: Ionospheric Rsch Lab

DEPARTMENT OF DEFENSE CONTRACTORS (Continued)

Photometrics, Inc
ATTN: I. Kofsky

Physical Dynamics, Inc
ATTN: J. Secan
ATTN: E. Fremouw

Physical Rsch, Inc
ATTN: R. Stephens
ATTN: R. Deliberis
ATTN: J. Devore
ATTN: K. Schwartz

R&D Associates
ATTN: G. Stoyr
ATTN: M. Gantsweg
ATTN: W. Karzas
ATTN: C. Greifinger
ATTN: F. Gilmore
ATTN: W. Wright
ATTN: R. Turco
ATTN: H. Ory
ATTN: P. Haas

R&D Associates
ATTN: B. Yoon

Rand Corp
ATTN: E. Bedrozian
ATTN: C. Crain

Riverside Rsch Institute
ATTN: V. Trapani

Rockwell International Corp
ATTN: R. Buckner

Rockwell International Corp
ATTN: S. Quilici

Science Applications, Inc
ATTN: D. Sachs
ATTN: D. Hamlin
ATTN: C. Smith
ATTN: L. Linson
ATTN: E. Straker

Science Applications, Inc
ATTN: J. Cockayne

Science Applications, Inc
ATTN: M. Cross

Stewart Radiance Lab
ATTN: J. Ulwick

Swerling, Manasse & Smith, Inc
ATTN: R. Manasse

Technology International Corp
ATTN: W. Boquist

DEPARTMENT OF DEFENSE CONTRACTORS (Continued)

SRI International
ATTN: A. Burns
ATTN: G. Price
ATTN: R. Tsunoda
ATTN: J. Vickrey
ATTN: V. Gonzales
ATTN: J. Petrickes
ATTN: M. Baron
ATTN: R. Livingston
ATTN: D. Neilson
ATTN: D. McDaniels
ATTN: W. Chesnut
ATTN: G. Smith
ATTN: W. Jaye
ATTN: R. Leadabrand
ATTN: C. Rino

Toyon Research Corp
ATTN: J. Ise
ATTN: J. Garbarino

DEPARTMENT OF DEFENSE CONTRACTORS (Continued)

TRW Electronics & Defense Sector
ATTN: G. Kirchner
ATTN: R. Plebuch

Utah State University
Attention Sec Con Ofc for
ATTN: A. Steed
ATTN: D. Burt
ATTN: K. Baker, Dir Atmos & Space Sci
ATTN: L. Jensen, Elec Eng Dept

VisiDyne, Inc
ATTN: W. Reidy
ATTN: J. Carpenter
ATTN: O. Shepard
ATTN: C. Humphrey